Joint Source Channel Anytime Coding Based on Spatially Coupled Repeat-Accumulate Codes

Li Deng, Xiaoxi Yu, Yixin Wang, Md. Noor-A-Rahim, Yong Liang Guan, *Senior Member, IEEE*, Zhiping Shi, *Member, IEEE*, and Zhongpei Zhang, *Member, IEEE*

***Abstract*— In our early work, we proposed a class of joint source channel anytime coding (JSCAC) scheme based on spatially coupled repeat-accumulate (SC-RA) codes, in addition to an improved partial joint expanding window decoding (PJEWD) algorithm. In this paper, we extend our preliminary results and make a comprehensive theoretical analysis for this system. First, we propose an improved density evolution (DE) algorithm for the SC-RA based JSCAC with PJEWD scheme. Based on the proposed DE algorithm, we systematically analyze the anytime property, the belief propagation (BP) decoding threshold, and the decoding complexity of this system over binary additive white Gaussian noise channel (BIAWGN), as well as the effects of code parameters on performances of the above three aspects. Moreover, we explore some application scenarios for JSCAC schemes, where it could maximize its advantages over the prior-art JSCC schemes. Both numerical and simulation results demonstrate the potentials of the proposed JSCAC scheme for high reliability and low latency communications. The proposed DE algorithm could also provide a good reference for the analysis of other JSCAC systems.**

***Index Terms*— Joint source channel coding (JSCC), anytime transmission, spatially coupled repeat-accumulate codes (SC-RA), expanding window decoding (EWD), density evolution (DE).**

Manuscript received 26 January 2023; revised 8 June 2023; accepted 3 August 2023. Date of publication 10 August 2023; date of current version 20 November 2023. This work was supported by the National Key Research and Development Program under Grant 2022YFC3005702; the Natural Science Foundation of Sichuan Province under Grant 2022NSFSC0488 and 2022NSFSC0489; the Natural Science Foundation of Guangxi Province under Grant 2022GXNSFBA035508, 2023GXNSFAA026018 and 2020GXNSFBA297018. The associate editor coordinating the review of this article and approving it for publication was L. Ong. *(Corresponding author: Zhiping Shi.)*

Li Deng is with the National Key Laboratory of Wireless Communications, University of Electronic Science and Technology of China, Chengdu 611731, China, and also with the School of Electronic Information and Automation, Guilin University of Aerospace Technology, Guilin 541004, China (e-mail: dengli@uestc.edu.cn).

Xiaoxi Yu and Yong Liang Guan are with the School of Electrical and Electronic Engineering, Nanyang Technological University, Singapore 639798 (e-mail: XIAOXI001@e.ntu.edu.sg; eylguan@ntu.edu.sg).

Yixin Wang is with the Institute for Infocomm Research (I2R), Agency for Science, Technology and Research (A*STAR), Singapore 138632 (e-mail: wang_yixin@i2r.a-star.edu.sg).

Md. Noor-A-Rahim is with the School of Computer Science and Information Technology, University College Cork, T12 XF62 Cork, Ireland (e-mail: m.rahim@cs.ucc.ie).

Zhiping Shi is with the National Key Laboratory of Wireless Communications, University of Electronic Science and Technology of China, Chengdu 611731, China, and also with the Yangtze Delta Region Institute (Huzhou), University of Electronic Science and Technology of China, Huzhou 611731, China (e-mail: szp@uestc.edu.cn).

Zhongpei Zhang is with the National Key Laboratory of Wireless Communications, University of Electronic Science and Technology of China, Chengdu 611731, China (e-mail: zhangzp@uestc.edu.cn).

Color versions of one or more figures in this article are available at https://doi.org/10.1109/TCOMM.2023.3303955.

Digital Object Identifier 10.1109/TCOMM.2023.3303955

I. Introduction

THE joint source channel coding (JSCC) is receiving renewed interests for communications in the non-asymptotic regime with delay constraints, owing to its lower complexity and higher fidelity compared to the traditional separate coding strategies [1]. The syndrome source coding structure of JSCC is suitable for asymmetric sources, such as uncompressed speech, text, and medical images, etc [2]. The asymmetric source can be measured with the source probability p, which is defined as the ratio of bits "1" in a binary source sequence. The error correction performance of JSCC system is not satisfactory for the source with relatively higher source probability (HSP) that does not match the source code rate. Moreover, if the source block-length is finite and relatively shorter, the error correction performance would be worse. On the other hand, anytime coding is effective for delay-sensitive and reliable communications [3]. The message block-lengths of anytime codes are relatively short to satisfy the delay constraints, while the expanding window decoding (EWD) and its optimized variants are adopted to ensure the communication reliability [4]. This paper discusses a novel JSCC scheme based on anytime coding techniques, which may provide new solutions for HSP source transmission in JSCC systems or anytime transmission of source streaming, etc. The prior-art works of JSCC and anytime coding, together with our contributions are detailed in this section.

A. State-of-the-Art of JSCC Schemes

Shannon's source channel separation coding theorem is the theoretical basis of modern communication systems. Considering the limitations of optimality assumptions of the separation coding theorem in practical applications, Shannon also pointed out the feasibility of joint source channel coding design [5]. Massey further proved that the JSCC structure can achieve the same or even better overall performance than the separate design by passing edge information between source and channel encoders or decoders, and the traditional separation coding design is only a special form of JSCC structure [1].

Among the prior-art JSCC schemes, the double low-density parity-check code (D-LDPC) based JSCC is a type of widely used block code based JSCC scheme, which performs the source encoding and channel encoding sequentially with two concatenated LDPC block codes, while decoding with the joint belief propagation (BP) decoder [6]. Authors of [7] first introduced protograph LDPC codes with merits of low decoding

thresholds and linear minimum distance growth [8] into the JSCC structure, called DP-LDPC codes. Successively, many variants of DP-LDPC codes are presented to further improve the error correction performance of JSCC systems with different optimization methods for the joint base matrix [9], [10], [11], [12], [13], [14], [15]. Recently, a new construction of JSCC scheme based on spatially coupled LDPC (SC-LDPC) codes and joint sliding window decoding is proposed in [16] and [17], outperforming the block code based JSCC schemes both in waterfall and error floor regions.

B. State-of-the-Art of Anytime Coding

Different from the classical coding theory which pursues error-free correction performance with the assumption of infinite coding delays, anytime transmission is designed for real-time reliable applications, such as tracking and control systems, etc [18]. The distinguishing features of anytime coding technique is concluded as: 1) Each short message block is encoded with causal spatial coupling pattern. 2) Each message block is decoded at any time instant with the expanding window structure or its variants. 3) The error probabilities exponentially decay with the decoding delay, and the parameter *delay-exponent* α is used to measure the decay speed.

The anytime transmission was first proved to be feasible with random tree codes [18], [19], which are non-linear and not well structured for practical applications. The emergence of anytime linear codes [20] set off a research boom for practical anytime codes. A type of classic practical anytime codes are constructed with protograph based low-density parity-check convolutional (LDPCC) codes [4], [21], [22], [23], which have fixed code structure and low encoder complexity. The anytime reliability of LDPCC codes is asymptotically attained by increasing the degrees of check node (CN) and variable node (VN) as time processes. Different from anytime LDPCC codes, anytime SC-LDPC codes introduced in [24] have fixed CN/VN degrees and random coupling structure, i.e., the connection probability between a VN and CN decays exponentially with their distance in a block chain, which can achieve better error correction performance than LDPCC anytime codes with fixed coupling structure. Authors in [24] also proposed an adaptive window decoding (AWD) to reduce the decoding complexity of traditional expanding window decoding (EWD) of anytime transmission [4]. Protograph based anytime spatially coupled repeat-accumulate (SC-RA) codes studied in [25] and [26] are variants of anytime SC-LDPC codes, both of which belong to channel error correction coding techniques without the source coding. Authors in [25] developed a protograph-based repeat-accumulate (P-RA) anytime code with fixed node degrees, and analyzed its anytime properties over the binary erasure channel (BEC) with the density evolution. In [26], the authors constructed a kind of anytime channel code based on SC-RA codes with variable node degrees, where the edge connection satisfies the exponential distribution. Moreover, the anytime properties of the proposed channel code are analyzed with the density evolution. As studied in [25] and [26], SC-RA codes outperform anytime SC-LDPC codes with lower encoding complexity in finite-length regime. These good features make SC-RA codes more suitable than SC-LDPC codes in linear anytime code designs [26], that is also the reason why SC-RA codes are adopted for joint source channel anytime coding in our work.

C. Contributions

We find that both the encoding and decoding structures of SC-RA anytime codes would be helpful to improve the error correction performance of JSCC systems. This key observation motivates us to improve the traditional JSCC schemes with anytime coding techniques. In the early version of this work [27], we constructed a hybrid joint source channel anytime coding (JSCAC) scheme based on SC-RA codes, in addition to an improved partial joint expanding window decoding (PJEWD) algorithm. In this paper, we extend our preliminary results and make a series of theoretical analysis for this system. The main contributions beyond [27] can be summarized as follows:

1) We present an improved density evolution (DE) analysis algorithm for the SC-RA based joint source and channel anytime coding (JSCAC) with partial joint extending window decoding (PJEWD) scheme [27], which also extends the density evolution algorithms in [24], [25], [26], and [28] for channel anytime SC-RA codes or channel anytime SC-LDPC codes.
2) Based on the proposed DE algorithm, we asymptotically analyze the SC-RA based JSCAC with PJEWD scheme over BIAWGN channel, including the anytime properties, the BP decoding threshold, and the decoding complexity. Moreover, a comprehensive study of the effects of code parameters on performances of the above three aspects is also performed.
3) We explore some applications of the proposed JSCAC scheme, including the finite-length source transmission with high source probability (HSP) and the source streaming transmission with jitter and jerkiness. Simulation results confirm its advantages in these scenarios over other prior-art JSCC schemes, as well as its potentials for real-time reliable applications.

D. Organization

The remainder of this paper is organized as follows. Section II provides some preliminaries of JSCC schemes, the anytime transmission and the anytime SC-RA code, in addition to our previous work in [27]. Section III describes the proposed density evolution algorithm and the asymptotic analysis for the SC-RA based JSCAC with PJEWD scheme. The simulation results and discussion are presented in Section IV, followed by conclusions in Section V.

II. Preliminaries

A. Block Code Based JSCC Scheme

Fig. 1 shows the classical Tanner graph of block LDPC based JSCC systems. The left and right sides represent the source LDPC code with the parity-check matrix of $\mathbf{H}_b^{sc}$ and the channel LDPC code with parity-check matrix of $\mathbf{H}_b^{cc}$, respectively. The black circle and rectangle represent

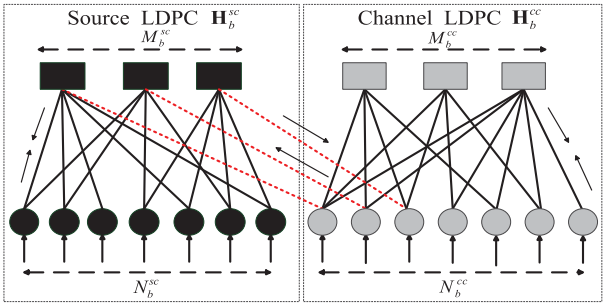

Fig. 1. Block LDPC based JSCC systems.

the source VN and corresponding syndrome node (SN); the gray circle and rectangle denote the channel VN and CN, respectively. The source SNs are connected with channel VNs one by one with a single public edge (red dashed lines in Fig. 1). Improved JSCC schemes also discuss the performance gains introduced by edge connections between source VNs and channel CNs [10], [14], [15]. Note that, for convenience of spatially coupling, the JSCC structure without source VN and channel CN connections as shown in Fig. 1 is adopted in the proposed scheme.

The concatenated source and channel encoding is implemented as follows. A source sequence $\mathbf{s}$ with block-length of N_b^{sc} is compressed by syndrome source coding as $\mathbf{u} = \mathbf{s}\mathbf{H}_b^{sc^T}$ with block-length of M_b^{sc}, thus the source block code rate is denoted as $R_b^{sc} = \frac{M_b^{sc}}{N_b^{sc}}$. Then the source syndrome $\mathbf{u}$ is further encoded with the channel generator matrix $\mathbf{G}_b^{cc}$. The channel codeword $\mathbf{x}$ with block-length of N_b^{cc} can be presented as $\mathbf{x} = \mathbf{u}\mathbf{G}_b^{cc} = (\mathbf{s}\mathbf{H}_b^{sc^T})\mathbf{G}_b^{cc}$. Accordingly, the channel block code rate is $R_b^{cc} = \frac{M_b^{sc}}{N_b^{cc}}$, and the overall block code rate is $R_b = \frac{R_b^{cc}}{R_b^{sc}} = \frac{N_b^{sc}}{N_b^{cc}}$.

The joint BP decoding performs the source BP decoder and channel BP decoder in parallel, exchanging the mutual information (MI) through the public edges (red dashed lines in Fig. 1). The initial log-likelihood-ratio (LLR) of source sequence is denoted by $Z^{sc} = \log\frac{1-p}{p}$, where p is the source probability; and the initial LLRs of received codeword $\mathbf{y}$ after binary-phase-shift-keying modulation (BPSK) and over BIAWGN channel is represented as $\mathbf{Z}^{cc} = \frac{2\mathbf{y}}{\sigma^2}$, where σ^2 is the variance of channel noise. See [6] for details of joint BP decoding algorithm.

B. Anytime Transmission

Fig. 2 shows the block diagram of communication system with anytime channel codes. Assume a source streaming produces a K-bit message block $\mathbf{u}_t \in \{0,1\}^K$ at each time instant t, which is encoded by the anytime channel encoder as a M-bit encoded message block $\mathbf{x}_t \in \{0,1\}^M$ with the code rate of $\frac{K}{M}$. The anytime channel encoder is defined by the function of $\mathbf{x}_t = E_t(\mathbf{U}_1^t)$, where $\mathbf{U}_1^t = [\mathbf{u}_1, \mathbf{u}_2, \ldots, \mathbf{u}_t]$. After the encoded message $\mathbf{x}_t$ is transmitted over a noisy channel, the receiver obtains its noise version $\mathbf{y}_t$. Then the anytime channel decoder estimates the current and all the previously received messages $\mathbf{U}_1^t$ at the time instant t, which can be described as $\hat{\mathbf{U}}_1^t(t) = D_t(\mathbf{y}_1^t)$, where $\mathbf{y}_1^t = [\mathbf{y}_1, \mathbf{y}_2, \ldots, \mathbf{y}_t]$ and $\hat{\mathbf{U}}_1^t = [\hat{\mathbf{u}}_1, \hat{\mathbf{u}}_2, \ldots, \hat{\mathbf{u}}_t]$. Denote the decoded error probability of i-th

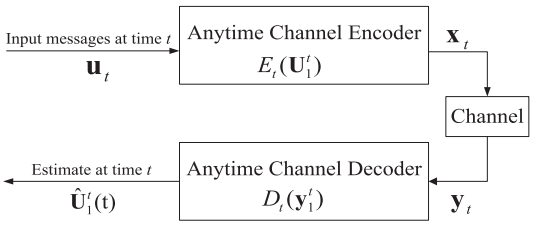

Fig. 2. Diagram of anytime communication.

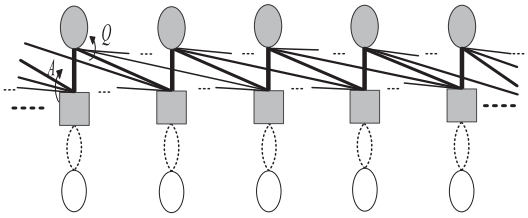

Fig. 3. Anytime SC-RA codes.

message $\mathbf{u}_i$ at time instant t as $P_e(i,t) = \Pr(\hat{\mathbf{u}}_i \neq \mathbf{u}_i)$, the definition of anytime code is shown below [19].

Definition 1: For a given channel, the encoder-decoder pair (E_t, D_t) is called anytime code if there exists $\alpha > 0$ such that

$$P_e(i,t) \leq \beta e^{-\alpha d}, \quad \forall d \neq 0, \tag{1}$$

where $d = t - i$ is the decoding delay of message $\mathbf{u}_i$, β is a positive constant describing the channel properties. The parameter α named *delay-exponent* describes the decay rate of $P_e(i,t)$, which is used to measure the anytime reliability. According to (1), α can be attained as [23]

$$\alpha \triangleq \lim_{d\to\infty}\left(\lim_{i\to\infty} -\frac{\log P_e(i,i+d)}{d}\right). \tag{2}$$

Definition 1 indicates that the error probability $P_e(i,t)$ of message $\mathbf{u}_i$ can exponentially decay to zero as the decoding delay d approaches to infinity, which is the key feature of anytime code. In practical anytime transmission systems, an estimated message is said to be reliable if its error probability is lower than a certain threshold, which is decided by specific applications [24].

C. Anytime SC-RA Codes

Authors in [29] first proposed a new class of spatially coupled codes based on regular RA protographs, which have several advantages over SC-LDPC codes including simpler encoders and slightly better thresholds than SC-LDPC codes with similar rates and decoding complexity. Authors in [26] further constructed a class of channel code for anytime communication based on SC-RA codes. Fig. 3 shows the Tanner graph of anytime SC-RA codes proposed in [26], where the gray and white circles represent the information bit node (IN) and parity bit node (PN), which have fixed degree of Q and 2, respectively. The gray rectangles indicate the CNs with fixed degree of A. The PNs are only connected to local CNs without coupling, in order to keep the simple coding structure of RA code, i.e., a cascade of low-density parity-check matrix and standard repeat-accumulator. Different from traditional SC-RA codes [29], the coupling mode of anytime SC-RA

codes must be causal, i.e., the INs of i-th message $\mathbf{u}_i$ must be independently connected to CNs of message $\mathbf{u}_j$, where $j \in [i, i+\gamma-1]$, and γ is the coupling length. Moreover, the exponential distribution of coupling edges is adopted instead of traditional uniform distribution to ensure a quickly recovery of recently received messages with small delay, which is a desired property for anytime codes [26]. The edge connection probabilities with exponential distribution is depicted with the line thickness in Fig. 3, which can also be written as [26]

$$P_r(k) = \frac{e^{-k\lambda}(1-e^{-\lambda})}{1-e^{-\gamma\lambda}}, \tag{3}$$

where λ is the exponential rate parameter, and $k = j - i$ is the distance between the connected IN and CN. The larger the parameter λ, the faster the error probability P_e decays as the decoding delay. When $\lambda = 0$, then $P_r(k) = 1$, which equals to the uniform distribution. The uniform distribution has a slow decline rate over the decoding delay, which is undesired in the anytime transmission. Other nonuniform distributions which have similar properties with the exponential distribution would also be suitable for the anytime transmission. Considering the generality and convenience for the theoretical analysis, the exponential distribution is adopted in this work.

The above mentioned code is referred to as (Q, A, λ, γ)-anytime SC-RA code, and the code rate is given by [29]

$$R = \frac{L}{L + \frac{Q}{A}(L - \gamma + 1 + 2(\gamma - \sum_{i=0}^{\gamma}(\frac{i}{\gamma})^A))}, \tag{4}$$

where L is the chain length.

D. Sketch of Joint Source Channel Anytime Coding Scheme

In this section, we briefly introduce our previous work in [27], including the hybrid coding structure of JSCAC scheme and the decoding strategies of PJEWD algorithm.

1) Coding Structure of JSCAC Scheme: The Tanner graph of the SC-RA based JSCAC scheme is shown in Fig. 4, where the SC-RA code is used as the skeleton. In Fig. 4, the upper half and lower half parts individually represent the source and channel codes. The black and gray circles indicate the source INs and channel INs with degrees of Q^{sc} and Q^{cc}; while the black and gray rectangles are source SNs and channel CNs with degrees of A^{sc} and A^{cc}, respectively. The PNs denoted by white circles are locally connected with fixed degree of 2. The source SNs are connected to channel VNs one by one with a single public edge for message passing. Both source and channel codes have exponential causal coupling structures with separate edge connection probabilities of P_r^{sc} and P_r^{cc}, followed as (3) with exponential rate of λ^{sc} and λ^{cc}, respectively. The code rate R^{cc} of $(Q^{cc}, A^{cc}, \lambda^{cc}, \gamma^{cc})$-channel code follows (4) with parameters of Q^{cc}, A^{cc} and γ^{cc}. Accordingly, the code rate R^{sc} of $(Q^{sc}, A^{sc}, \lambda^{sc}, \gamma^{sc})$-source code is

$$R^{sc} = 1 - \frac{L}{L + \frac{Q^{sc}}{A^{sc}}(L - \gamma^{sc} + 1 + 2(\gamma^{sc} - \sum_{i=0}^{\gamma^{sc}}(\frac{i}{\gamma^{sc}})^{A^{sc}}))}. \tag{5}$$

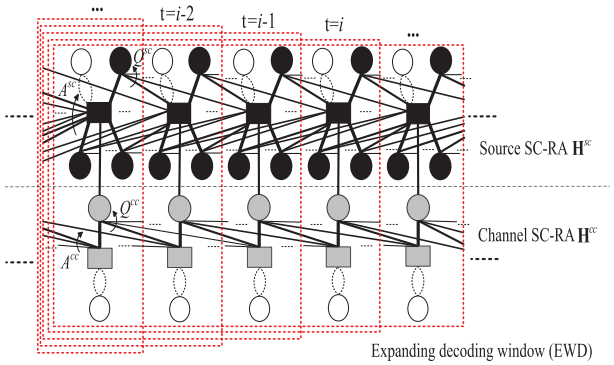

Fig. 4. SC-RA based JSCAC scheme.

As $L \to \infty$, the asymptotic code rates become as $R^{cc} \to \frac{A^{cc}}{A^{cc}+Q^{cc}}$, $R^{sc} \to \frac{Q^{sc}}{A^{sc}+Q^{sc}}$, which are equal to the channel block code rate R_b^{cc} and the source block code rate R_b^{sc}, respectively.

The SC-RA based JSCAC scheme follows the concatenated syndrome source encoding and channel encoding structure of block LDPC based JSCC systems. See [27] for details.

2) Partial Joint Expanding Window Decoding (PJEWD): The expanding window decoding (EWD) technique [4] is adopted in the JSCAC scheme. The red dashed rectangles in Fig. 4 represent the decoding windows expanded with the decoding delay, meanwhile the dimensions of source and channel parity-check matrices are also expanded accordingly. In each decoding window, the joint BP decoding [6] is implemented on the involved message blocks. However, the decoding complexity of EWD (specially for BP decoding) grows linearly with the decoding delay [26]. On the other hand, it is observed that the source and channel BP decoders in block LDPC based JSCC systems have unequal convergence rates, i.e., the channel decoding converges faster than source decoding [30]. The convergence inconsistency would result in error propagation from source blocks to channel blocks through public edges, leading to a higher error floor. In order to alleviate this phenomenon and reduce the decoding complexity, a partial joint expanding window decoding (PJEWD) algorithm was proposed in [27], which are generalized as:

- For the joint BP decoding at each time instant t, once the channel decoding convergence is detected, stop message updating for all the channel nodes, while keeping message updating for the source nodes with the mutual information from the channel decoder.
- At each time instant t, calibrate the estimated result of early transmitted source message blocks $\mathbf{s}_{[1,t-1]}$ by updating the a posterior $\mathbf{LLR}_t^{sc}$ in the current decoding delay with the corresponding a posterior $\mathbf{LLR}_{t-1}^{sc}$ in the last time instant before the hard decision. The calibrate decoding result of $\mathbf{s}_{[1,t-1]}$ at time instant t is detailed as $\hat{\mathbf{s}}_{[1,t-1]} = (-\text{sign}(\mathbf{LLR}_{t-1}^{sc} + \mathbf{LLR}_t^{sc}) + 1)/2, \quad t \in (1, L]$.

The first strategy is designed to lower the probability of transmitting the unreliable information from the source nodes to channel nodes that in turns disturbing the convergent status of channel decoder. In addition, the partial updating could reduce the decoding complexity by skipping the message updates for the convergent nodes. The second strategy is designed to

further improve the bit error rate (BER) performance of source decoding. It is found that updating the current decoded source information by adding on the previously well decoded source information can effectively improve the BER performance of JSCAC codes with finite coupling length.

III. Asymptotic Analysis of JSCAC Scheme

Different from the density evolution (DE) algorithms in [25] and [26] which are designed to analyze the anytime properties of channel SC-RA codes, we present the improved DE algorithm for the proposed SC-RA based joint source channel anytime coding (JSCAC) with PJEWD scheme over BIAWGN channel. Moreover, the proposed DE algorithm can not only analyze the anytime property of proposed code, but also the BP decoding threshold and decoding complexity.

A. Density Evolution Process of JSCAC Scheme

The Gaussian approximation [31] is adopted to implement the density evolution on BP algorithm, where the Gaussian LLR message with $\mathcal{N}(\mu,\sigma^2)$ $(\sigma^2=2\mu)$ is considered. Before that, some notations are defined as:

- $x_{sv}^l(i_s,t)(x_{cv}^l(i_c,t))$: message exchange from source IN_{i_s}(channel IN_{i_c}) to connected source SNs (channel CNs) at l-th iteration and time t;
- $\tilde{x}_{cv}^l(i_c,t)$: message exchange from channel IN_{i_c} to source SN_{j_s} at l-th iteration and time t;
- $x_{sp}^l(j_s,t)(x_{cp}^l(j_c,t))$: message exchange from source PN_{j_s} (channel PN_{j_c}) to source SN_{j_s} (channel CN_{j_c}) at l-th iteration and time t;
- $y_{sv}^l(j_s,t)(y_{cv}^l(j_c,t))$: message exchange from source SN_{j_s} (channel CN_{j_c}) to connected source (channel) INs at l-th iteration and time t;
- $\tilde{y}_{sv}^l(j_s,t)$: message exchange from source SN_{j_s} to channel IN_{i_c} at l-th iteration and time t;
- $y_{sp}^l(j_s,t)(y_{cp}^l(j_c,t))$: message exchange from source SN_{j_s} (channel CN_{j_c}) to source PN_{j_s} (channel PN_{j_c}) at l-th iteration and time t;

Fig. 5 also shows the message updates in the joint Tanner graph of SC-RA based JSCAC scheme. In Fig. 5 and above notations, i_s and i_c denote the index of certain source and channel IN node, respectively; j_s represents the location of certain connected source SN node and source PN node; j_c represents the location of certain connected channel CN node and channel PN node. According to the encoding and decoding structure of SC-RA based JSCAC with PJEWD scheme shown in Section II-D, the corresponding density evolution process is detailed as follows. Thereinto, the channel updating equations are mainly referenced from [26], and the message exchanging patterns between the source and channel parts, in addition to the error probability calculation are referenced from [6].

Step 1: Initialize the parameters of the maximum iteration number l_{max}, λ^{sc}, λ^{cc}, γ^{sc}, γ^{cc}, then P_r^{sc} and P_r^{cc} are derived from (3), and initialize $x_{cv}^0(i_c,t)=x_{cp}^0(j_c,t)=\mu_0=\frac{2}{\sigma_n^2}$, $0<i_c,j_c\le t$, where σ_n is the given channel noise variance; $x_{sv}^0(i_s,t)=x_{sp}^0(j_s,t)=\nu_0=\log\frac{1-p}{p}$, $0<i_s,j_s\le t$, where p is the given source probability. Initialize the channel node update sign as $Tag_c=1$, the number of message updates as $Num_{me}=0$, and the number of iterations as $l=0$.

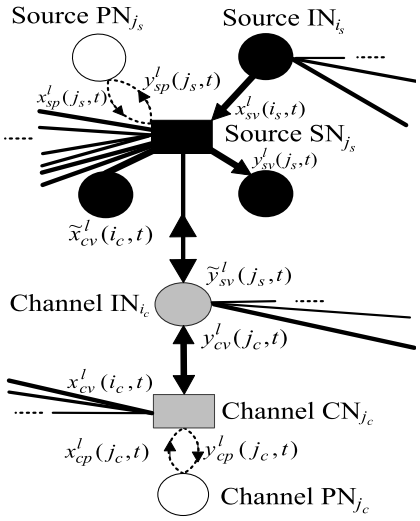

Fig. 5. Message updates in the joint Tanner graph of SC-RA based JSCAC scheme.

Step 2: If $Tag_c=1$, update channel nodes with (6) to (10), and update Num_{me}.

- channel CNs update:

$$\begin{aligned} y_{cv}^l(j_c,t) &= \Phi^{-1}\Bigg\{1 \\ &\quad-\left[1-\Phi\left(J^{-1}\left(\sum_{k=0}^{\infty}P_r^{cc}(k)J\left(x_{cv}^l(j_c-k,t)\right)\right)\right)\right]^{A^{cc}-1} \\ &\quad\cdot\left[1-\Phi\left(x_{cp}^l(j_c,t)\right)\right]^2\Bigg\}, \end{aligned} \tag{6}$$

$$\begin{aligned} y_{cp}^l(j_c,t) &= \Phi^{-1}\Bigg\{1 \\ &\quad-\left[1-\Phi\left(J^{-1}\left(\sum_{k=0}^{\infty}P_r^{cc}(k)J\left(x_{cv}^l(j_c-k,t)\right)\right)\right)\right]^{A^{cc}} \\ &\quad\cdot\left[1-\Phi\left(x_{cp}^l(j_c,t)\right)\right]\Bigg\}, \end{aligned} \tag{7}$$

- channel PNs update:

$$x_{cp}^{l+1}(j_c,t)=\mu_0+y_{cp}^l(j_c,t), \tag{8}$$

- channel INs update:

$$\begin{aligned} x_{cv}^{l+1}(i_c,t) &= \mu_0+(Q^{cc}-1) \\ &\quad\cdot J^{-1}\left(\sum_{j_c=0}^{t-i_c}P_r^{cc}(j_c)J\left(y_{cv}^l(i_c+j_c,t)\right)\right) \\ &\quad+J^{-1}\left(J\left(\tilde{y}_{sv}^l(j_s,t)\right)\right), \end{aligned} \tag{9}$$

$$\tilde{x}_{cv}^{l+1}(i_c,t)=\mu_0+Q^{cc}$$

$$\cdot J^{-1}\Big(\sum_{j_c=0}^{t-i_c} P_r^{cc}(j_c)J\big(y_{cv}^l(i_c+j_c,t)\big)\Big), \tag{10}$$

Step 3: Update the source nodes with (11) to (15), and update Num_{me}.

- source SNs update:

$$\begin{aligned} &y_{sv}^l(j_s,t)\\ &=\Phi^{-1}\Bigg\{1\\ &\quad-\left[1-\Phi\left(J^{-1}\left(\sum_{k=0}^{\infty}P_r^{sc}(k)J\left(x_{sv}^l(j_s-k,t)\right)\right)\right)\right]^{A^{sc}-1}\\ &\quad\cdot\left[1-\Phi\left(x_{sp}^l(j_s,t)\right)\right]^2\cdot\left[1-\Phi\left(\tilde{x}_{cv}^l(j_c,t)\right)\right]\Bigg\}, \end{aligned} \tag{11}$$

$$\begin{aligned} &\tilde{y}_{sv}^l(j_s,t)\\ &=\Phi^{-1}\Bigg\{1\\ &\quad-\left[1-\Phi\left(J^{-1}\left(\sum_{k=0}^{\infty}P_r^{sc}(k)J\left(x_{sv}^l(j_s-k,t)\right)\right)\right)\right]^{A^{sc}}\\ &\quad\cdot\left[1-\Phi\left(x_{sp}^l(j_s,t)\right)\right]^2\Bigg\}, \end{aligned} \tag{12}$$

$$\begin{aligned} &y_{sp}^l(j_s,t)\\ &=\Phi^{-1}\Bigg\{1\\ &\quad-\left[1-\Phi\left(J^{-1}\left(\sum_{k=0}^{\infty}P_r^{sc}(k)J\left(x_{sv}^l(j_s-k,t)\right)\right)\right)\right]^{A^{sc}}\\ &\quad\cdot\left[1-\Phi\left(x_{sp}^l(j_s,t)\right)\right]\cdot\left[1-\Phi\left(\tilde{x}_{cv}^l(j_c,t)\right)\right]\Bigg\}, \end{aligned} \tag{13}$$

- source PNs update:

$$x_{sp}^{l+1}(j_s,t)=\nu_0+y_{sp}^l(j_s,t), \tag{14}$$

- source INs update:

$$\begin{aligned} &x_{sv}^{l+1}(i_s,t)\\ &=\nu_0+(Q^{sc}-1)\\ &\quad\cdot J^{-1}\Big(\sum_{j_s=0}^{t-i_s}P_r^{sc}(j_s)J_{\mathrm{BSC}}\big(y_{sv}^l(i_s+j_s,t),p\big)\Big), \end{aligned} \tag{15}$$

where

$$\begin{aligned} &\Phi(\mu)\\ &=\begin{cases}1-\dfrac{1}{\sqrt{4\pi\mu}}\displaystyle\int_{-\infty}^{\infty}(\tanh(\frac{\mu}{2}))e^{-\frac{(\xi-\mu)^2}{4\mu}}\mathrm{d}\xi, & if\ \mu>0\\ 1, & if\ \mu=0\end{cases}\\ &J(\mu)\\ &=1-\frac{1}{\sqrt{4\pi\mu}}\int_{-\infty}^{\infty}(e^{-\frac{(\xi-\mu)^2}{4\mu}}\log_2(1+e^{-\xi})\mathrm{d}\xi,\\ &J_{\mathrm{BSC}}(\mu,p)\\ &=(1-p)I(V;\chi^{(1-p)})+pI(V;\chi^p), \end{aligned}$$

where $I(V;\chi^{(1-p)})$ ($I(V;\chi^p)$) denotes the mutual information between source INs and $\chi^{(1-p)}$ (χ^p), and $\chi^{(1-p)}\sim\mathcal{N}(\mu+\nu_0,2\mu)$, $\chi^p\sim\mathcal{N}(\mu-\nu_0,2\mu)$ [6].

Step 4: Update $x_{sv}^l(i_s,t-1)=\frac{1}{2}[x_{sv}^l(i_s,t-1)+x_{sv}^l(i_s,t)]$, $t\in(1,L]$;

Step 5: If $|x_{cv}^{l+1}(i_c,t)-x_{cv}^l(i_c,t)|==0, 0<i_c\le t$, update $Tag_c=0$;

Step 6: If (16) is satisfied, output the decoding threshold as:

$$\begin{aligned} \frac{E_b}{N_0}^* &=\inf\Big\{\frac{E_b}{N_0}:\lim_{l,L\to\infty}x_{cv}^l(i_c,t),x_{sv}^l(i_s,t),\\ &\qquad x_{cp}^l(j_c,t),x_{sp}^l(j_s,t)=\infty,\quad\forall i_c,i_s,j_c,j_s,t\Big\}. \end{aligned} \tag{16}$$

See detailed discussion about (16) in Section III-C and Appendix in Section VI-A.

Step 7: If $l<l_{max}$, then $l=l+1$ and turn to Step 2; Otherwise, stop DE process and calculate the error probability $P_e(i_s,t)$ of source IN_{i_s} at the time t and the maximum iteration number of $l_{\max}$ as [6]:

$$\begin{aligned} &P_e(i_s,t)\\ &=Q^{sc}\big[p\mathcal{Q}_f\big(X_{sv}^p(i_s,t)\big)+(1-p)\mathcal{Q}_f\big(X_{sv}^{(1-p)}(i_s,t)\big)\big], \end{aligned} \tag{17}$$

where $\mathcal{Q}_f(x)=\frac{1}{\sqrt{2\pi}}\int_x^{\infty}e^{-\frac{\xi^2}{2}}d\xi$, and

$$\begin{aligned} X_{sv}^p(i_s,t)&=\sqrt{\frac{U_{sv}(i_s,t)}{2}}-\frac{\nu_0}{\sqrt{2U_{sv}(i_s,t)}},\\ X_{sv}^{(1-p)}(i_s,t)&=\sqrt{\frac{U_{sv}(i_s,t)}{2}}+\frac{\nu_0}{\sqrt{2U_{sv}(i_s,t)}},\\ U_{sv}(i_s,t)&=\nu_0+Q^{sc}\\ &\quad\cdot J^{-1}\Big(\sum_{j_s=0}^{t-i_s}P_r^{sc}(j_s)J_{\mathrm{BSC}}\big(y_{sv}^{l_{\max}}(i_s+j_s,t),p\big)\Big). \end{aligned}$$

B. Asymptotic Anytime Properties Analysis

Based on the above DE analysis, we can discuss the anytime properties of the proposed codes. The lower bound of *delay-exponent* is provided in the following theorem.

Theorem 1: Consider the SC-RA based joint source channel anytime code (JSCAC) referred to as anytime $(Q^{sc},A^{sc},\lambda^{sc},\gamma^{sc},Q^{cc},A^{cc},\lambda^{cc},\gamma^{cc})$ code over BIAWGN channel, the *delay-exponent* α satisfies

$$\alpha\ge 0.4325\lambda^{sc}Q^{sc}. \tag{18}$$

We prove **Theorem 1** based on the following facts: (a) $x_{cv}^{\infty}(i_c,t)=+\infty$, $x_{sv}^{\infty}(i_s,t)=+\infty$, $x_{cp}^{\infty}(j_c,t)=+\infty$, $x_{sp}^{\infty}(j_s,t)=+\infty$, $\forall 0<i_c,i_s,j_c,j_s\le t$, $\frac{E_b}{N_0}>\frac{E_b}{N_0}^*$. The

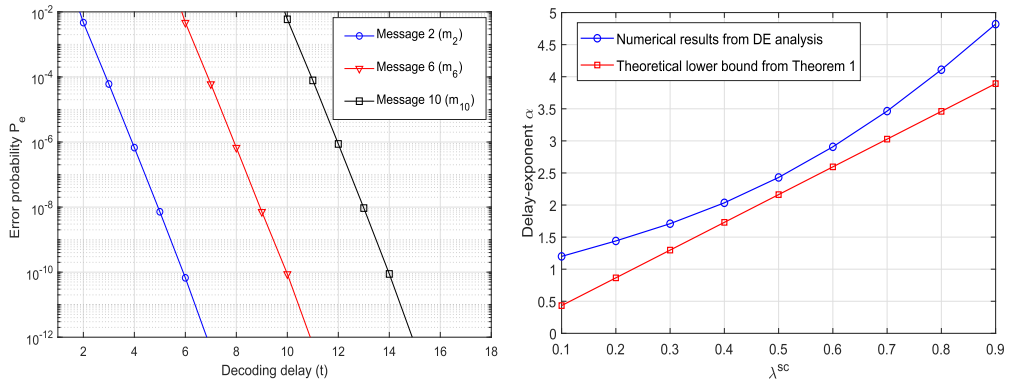

(a) (b)

Fig. 6. Asymptotic anytime properties of the proposed $(10, 10, 0.5, 10, 10, 10, 0.1, 10)$ code with $L = \infty$, $p = 0.04$, and $\frac{E_b}{N_0} = 0$ dB: (a) the error probabilities of message blocks as the decoding delay; (b) *Delay-exponent* comparison between numerical results and theoretical lower bounds.

derivation of claim (a) is detailed in Appendix; (b) For $\Phi(\cdot)$ function, $\Phi(+\infty) = 0$, and $\Phi^{-1}(0) = +\infty$; For $J(\cdot)$ function, $J(+\infty) = 1$, and $J^{-1}(1) = +\infty$; For $J_{\mathrm{BSC}}(\cdot)$ function, $J_{\mathrm{BSC}}(+\infty) = 1$; (c) The approximation of $J^{-1}(\cdot)$ in [32] is adopted; (d) $\mathcal{Q}(\mu) \leqslant e^{-\frac{\mu^2}{2}}$, for $\mu \geqslant 0$.

Accordingly, as $l \to \infty$, $y_{sv}^l(j_s, t)$ in (11) becomes as

$$\begin{aligned}\lim_{l\to\infty} y_{sv}^l(j_s,t) &\overset{(a),(b)}{=} \Phi^{-1}\Bigg\{1 \\ &\quad - \left[1 - \Phi\left(J^{-1}\left(\sum_{k=0}^{\infty} P_r^{sc}(k)\cdot 1\right)\right)\right]^{A^{sc}-1} \\ &\quad \cdot [1-0]^2 \cdot [1-0]\Bigg\} \\ &= \Phi^{-1}\left\{1 - [1-0]^{A^{sc}-1}\right\} \\ &= +\infty, \end{aligned} \tag{19}$$

and $U_{sv}(i_s, t)$ in (17) can be presented as

$$\begin{aligned}\lim_{l\to\infty} U_{sv}(i_s,t) &\overset{(a),(b)}{=} \nu_0 + Q^{sc}\cdot J^{-1}\left(\sum_{j_s=0}^{t-i_s} P_r^{sc}(j_s)\cdot 1\right) \\ &= \nu_0 + Q^{sc}\cdot J^{-1}\left(\sum_{k=0}^{d} P_r^{sc}(k)\right) \\ &= \nu_0 + Q^{sc}\cdot J^{-1}\left(1 - e^{-\lambda^{sc}(d+1)}\right) \\ &\overset{(c)}{\approx} \nu_0 + Q^{sc}\cdot 0.5\left[0.7\lambda^{sc}(d+1)\right. \\ &\qquad \left. +2.42 - 1.75e-\lambda^{sc}(d+1)\right]^2 \\ &= 1.694\lambda^{sc}Q^{sc}(d+1) + Z_0, \end{aligned} \tag{20}$$

where $Z_0 = \nu_0 + 0.245Q^{sc}(\lambda^{sc})^2(d+1)^2 + 2.928Q^{sc} + 1.531Q^{sc}e^{-2\lambda^{sc}(d+1)} - 4.235Q^{sc}e^{-\lambda^{sc}(d+1)} - 1.225Q^{sc}\lambda^{sc}(d+1)e^{-\lambda^{sc}(d+1)}$. Since

$$\begin{aligned}\mathcal{Q}_f\left(X_{sv}^{p}(i_s,t)\right) &\overset{(d)}{\leq} e^{-\frac{(X_{sv}^{p}(i_s,t))^2}{2}} \\ &= e^{-\frac{1}{2}\left(\frac{U_{sv}(i_s,t)}{2} - \nu_0 + \frac{\nu_0^2}{2U_{sv}(i_s,t)}\right)} \\ &\leq e^{\left(-\frac{U_{sv}(i_s,t)}{4} + \frac{\nu_0}{2}\right)}, \end{aligned} \tag{21}$$

$$\begin{aligned}\mathcal{Q}_f\left(X_{sv}^{(1-p)}(i_s,t)\right) &\overset{(d)}{\leq} e^{-\frac{(X_{sv}^{(1-p)}(i_s,t))^2}{2}} \\ &= e^{-\frac{1}{2}\left(\frac{U_{sv}(i_s,t)}{2} + \nu_0 + \frac{\nu_0^2}{2U_{sv}(i_s,t)}\right)} \\ &\leq e^{\left(-\frac{U_{sv}(i_s,t)}{4} - \frac{\nu_0}{2}\right)}, \end{aligned} \tag{22}$$

thus the error probability of (17) can be described as

$$\begin{aligned}P_e(i_s,t) &\leq Q^{sc}\left[pe^{\left(-\frac{U_{sv}(i_s,t)}{4}+\frac{\nu_0}{2}\right)} + (1-p)e^{\left(-\frac{U_{sv}(i_s,t)}{4}-\frac{\nu_0}{2}\right)}\right] \\ &\overset{\nu_0=\log\frac{1-p}{p}}{=} 2Q^{sc}\sqrt{p(1-p)}e^{-\frac{U_{sv}(i_s,t)}{4}}. \\ &\overset{(20)}{\approx} 2Q^{sc}\sqrt{p(1-p)}e^{-\frac{1}{4}[1.694\lambda^{sc}Q^{sc}(d+1)+Z_0]} \\ &= \beta e^{-0.4325\lambda^{sc}Q^{sc}d}, \end{aligned} \tag{23}$$

where $\beta = 2Q^{sc}\sqrt{p(1-p)}e^{(-0.4325\lambda^{sc}Q^{sc}-0.25Z_0)}$, and $\beta > 0$. Accordingly, the $delay-exponent$ α can be attained by replacing (23) into (2) as $\alpha \geq 0.4325\lambda^{sc}Q^{sc}$.

As shown in (23) that, the proposed SC-RA based JSCAC code has exponentially decay of error probability as the decoding delay with positive $\alpha \geq 0.4325\lambda^{sc}Q^{sc}$. According to **Definition 1**, we can conclude that it is anytime decodable over BIAWGN channel, which is referred to as anytime $(Q^{sc}, A^{sc}, \lambda^{sc}, \gamma^{sc}, Q^{cc}, A^{cc}, \lambda^{cc}, \gamma^{cc})$ code. ■

Fig. 6 shows the asymptotic anytime properties of proposed (10, 10, 0.5, 10, 10, 10, 0.1, 10) code. It can be observed in Fig. 6(a) that, the error probabilities of different message blocks (m_2, m_6 and m_{10}) exponentially decay with the decoding delay, which are time-shifted versions of each other. From the slopes of the error probability curves, we can numerically derive the *delay-exponent* α. Fig. 6(b) verifies the correctness of **Theorem 1** by comparing the theoretical lower bound of the *Delay-exponent* α from **Theorem 1** and the DE analysis result. As seen in Fig. 6(b), the theoretical lower bound is close to the DE analysis result with a certain gap. This gap is caused by the approximation in (20) and the scaling processes in (21) and (22) that occurred in the derivation of the theoretical lower bound. Moreover, from (18), α can linearly increase with the increment of λ^{sc} (or Q^{sc}). A larger α can make a faster decay of error probability, but may result in an error floor at large decoding delays [24]. Therefore, a moderate λ^{sc} or Q^{sc} might be suitable for the finite-length source transmission.

Fig. 7 shows the effects of code parameters on the asymptotic anytime properties, where the x-axis represents the decoding delay t and y-axis is the error probability p_e. Note

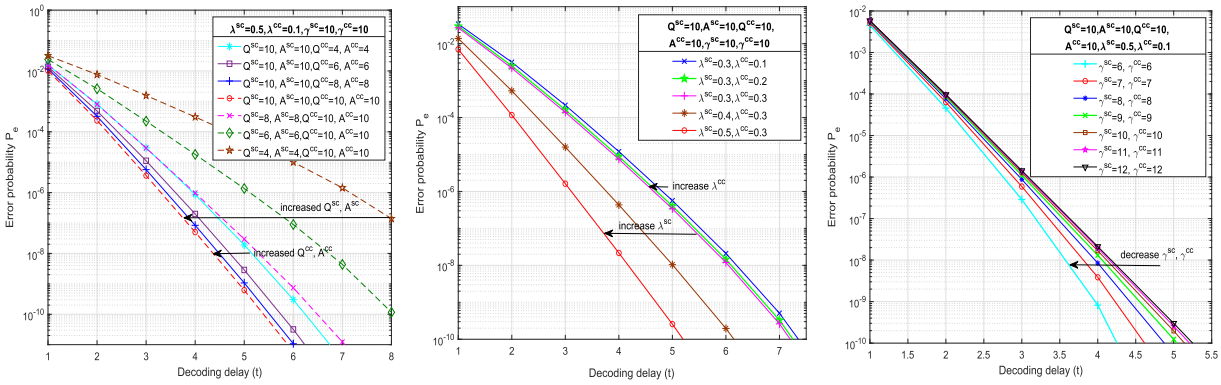

(a) (b) (c)

Fig. 7. Effects of code parameters on the asymptotic anytime properties with $p = 0.04$, $\frac{E_b}{N_0} = 0$ dB: (a) effects of node degrees; (b) effects of exponential rates; (c) effects of coupling lengths.

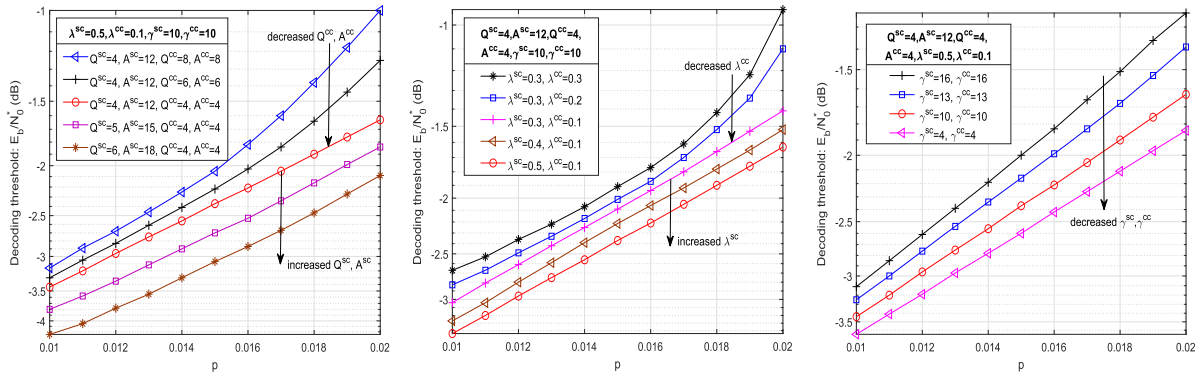

(a) (b) (c)

Fig. 8. Effects of code parameters on the asymptotic BP decoding threshold: (a) effects of node degrees; (b) effects of exponential rates; (c) effects of coupling lengths.

that, for the sake of easy storage, we choose to equate the source and channel coupling lengths, i.e., $\gamma^{sc} = \gamma^{sc}$ (the same as below). It can be seen in Fig. 7(a) and Fig. 7(b) that both increasing the node degrees and the exponential rates can lead to a larger slope of the error probability curve. Moreover, the source code parameters have larger effects than corresponding channel parameters. Fig. 7(c) indicates that a smaller coupling length leads to a larger slope of the error probability curve. As the increase of coupling lengths, the differences of curve slopes become smaller.

C. Asymptotic BP Decoding Threshold Analysis

Authors in [33] proposed a generalized Shannon theorem for JSCC systems, i.e., the theoretical limit of code rate for the transmission of an asymmetric source over AWGN channel as follows:

$$H(p)\frac{R^{cc}}{R^{sc}} < \frac{1}{2}\log_2\left(1+\frac{2E_s}{N_0}\right), \tag{24}$$

where $\frac{R^{cc}}{R^{sc}}$ is the overall code rate; $H(p)$ is the source entropy calculated by $H(p) = -p\log_2 p - (1-p)\log_2(1-p)$; E_s is the average energy per symbol transmitted through the channel, and N_0 is defined as $N_0 = 2\sigma_n^2$. For BPSK modulated BIAWGN channel, the ratio of bit energy to noise power spectral density $\frac{E_b}{N_0}$ is used to measure the channel condition in this paper.

For a given p, the BP decoding threshold $\frac{E_b}{N_0}^*$ of an anytime $(Q^{sc}, A^{sc}, \lambda^{sc}, \gamma^{sc}, Q^{cc}, A^{cc}, \lambda^{cc}, \gamma^{cc})$ code is defined as the minimum $\frac{E_b}{N_0}$, which can make the messages exchange from source IN_{i_s} (channel IN_{i_c}) to connected source SNs (channel CNs) at time instant t approach to infinity with infinite iterations and chain length (see (16) in Section III-A).

Based on the proposed DE algorithm, the effects of code parameters on the BP decoding threshold can be explored. Fig. 8(a) shows how the node degrees influence the decoding threshold, where the x-axis represents the source probability p. It can be seen that bigger source node degrees but smaller channel node degrees can lead to lower decoding thresholds. Moreover, the source node degrees have greater effects than channel node degrees, especially in the small source probability region. In Fig. 8(b), the effects of exponential rates are similar with node degrees, i.e., decreased λ^{cc} but increased λ^{sc} result in lower decoding thresholds. While Fig. 8(c) indicates that smaller coupling lengths can achieve better decoding thresholds. However, a too small coupling length would potentially lead to a higher error floor, especially for finite-length codes.

Table I and Table II compare the BP decoding thresholds of different code ensembles. We keep comparable node degrees and coupling lengths with regular SC-LDPC codes in [17]. Note that, the coupling lengths (γ^{sc} and γ^{cc}) and the memories (m_s and m_c) in [17] satisfy the relations of $\gamma^{sc} = m_s + 1$ and $\gamma^{cc} = m_c + 1$, by comparing the base matrix in Eq. (10) of [17] and the parity-check matrix in Eq. (4) of [27]. For DP-LDPC based JSCC schemes in [9], [12], and [14], the optimized base matrices with irregular node degrees are marked. In Table I,

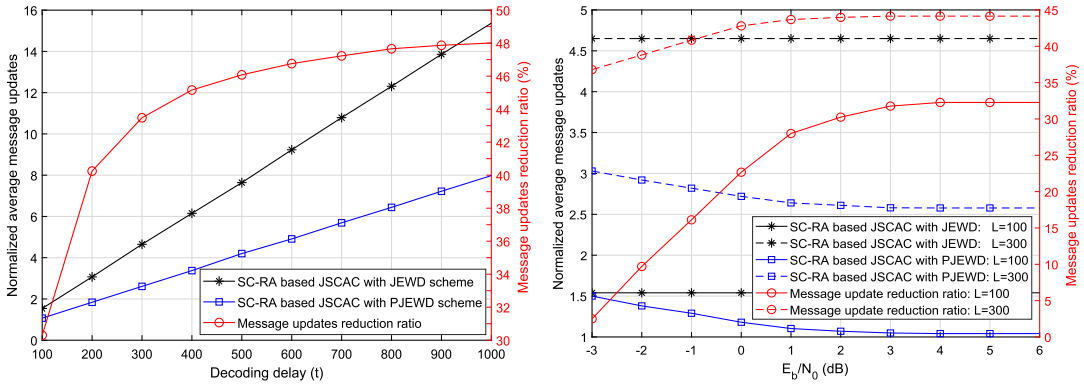

(a) (b)

Fig. 9. Asymptotic decoding complexity of the anytime (4, 12, 0.5, 3, 3, 3, 0.1, 3) code: (a) normalized average message updates as the decoding delay ($\frac{E_b}{N_0} = 2$ dB); (b) normalized average message updates as the channel condition. The average message updates are normalized by the (3,12)- and (3,6)-regular LDPC based JSCC scheme [6], the same in Fig. 10.

TABLE I

BP DECODING THRESHOLD $\frac{E_b}{N_0}^*$ (dB) FOR DIFFERENT CODES WITH $R^{sc} = 0.25$ AND $R^{cc} = 0.5$

Code Ensemble	$p = 0.01$	$p = 0.02$
block DP-LDPC based JSCC: $\mathbf{B}_{\mathrm{AR4JA}}$ [9]	-2.524	-0.632
block DP-LDPC based JSCC: $\mathbf{B}_{\mathrm{AR3A}}$ [9]	-3.248	-0.965
block DP-LDPC based JSCC: $\mathbf{B}_{\mathrm{IARA}-2}$ [9]	-3.438	-1.379
(3, 12)-and (3, 6)-regular SC-LDPC code: $m_s = 2, m_c = 2, W = 20$ [17]	-3.645	-1.569
proposed (4, 12, 0.5, 3, 4, 4, 0.1, 3) code: $\gamma^{sc} = 3, \gamma^{cc} = 3$	-3.68	-1.87
Shannon limit	-5.97	-3.14

TABLE II

BP DECODING THRESHOLD $\frac{E_b}{N_0}^*$ (dB) FOR DIFFERENT CODES WITH $R^{sc} = 0.5$ AND $R^{cc} = 0.5$

Code Ensemble	$p = 0.04$	$p = 0.06$
block DP-LDPC based JSCC: ($\mathbf{B}_{s1}$, $\mathbf{B}_{c1}$) [12]	-2.10	–
block DP-LDPC based JSCC: ($\mathbf{B}_{s2}$, $\mathbf{B}_{c1}$) [12]	–	-0.8
block DP-LDPC based JSCC: $\mathbf{B}_J^{opti\text{-}4}$ [14]	-2.577	–
(3, 6)- and (3, 6)-regular SC-LDPC code: $m_s = 2, m_c = 2, W = 20$ [17]	-2.54	-1.34
(4, 8)- and (3, 6)-regular SC-LDPC code: $m_s = 3, m_c = 2, W = 20$ [17]	-2.86	-1.62
(5, 10)- and (3, 6)-regular SC-LDPC code: $m_s = 4, m_c = 2, W = 20$ [17]	-3.05	-1.75
proposed (4, 4, 0.5, 3, 4, 4, 0.1, 3) code: $\gamma^{sc} = 3, \gamma^{cc} = 3$	-1.95	-0.73
proposed (6, 6, 0.5, 4, 4, 4, 0.1, 3) code: $\gamma^{sc} = 4, \gamma^{cc} = 3$	-3.36	-1.90
proposed (8, 8, 0.5, 5, 4, 4, 0.1, 3) code: $\gamma^{sc} = 5, \gamma^{cc} = 3$	-3.82	-2.11
Shannon limit	-4.02	-2.36

the source and channel code rates are $R^{sc} = \frac{1}{4}$ and $R^{cc} = \frac{1}{2}$. It can been seen that the decoding thresholds of anytime (4, 12, 0.5, 3, 4, 4, 0.1, 3) code with $\gamma^{sc} = \gamma^{cc} = 3$ outperforms block DP-LDPC based JSCC schemes and has lower decoding thresholds than (3,12)- and (3,6)-regular SC-LDPC code [17] with $m_s = m_c = 2$ and $W = 20$, especially at higher source probability of $p = 0.02$. Table II compares the BP decoding thresholds of code ensembles with $R^{sc} = \frac{1}{2}$ and $R^{cc} = \frac{1}{2}$. It can been seen that the anytime (4, 4, 0.5, 3, 4, 4, 0.1, 3) code with source node degrees of $Q^{sc} = A^{sc} = 4$ has the worst decoding thresholds compared with the codes in [12], [14], and [17]. While the anytime (6, 6, 0.5, 4, 4, 4, 0.1, 3) codes and (8, 8, 0.5, 5, 4, 4, 0.1, 3) codes with higher source node degrees of $Q^{sc} = A^{sc} = 6$ and 8 can further achieve lower BP decoding thresholds than (4, 8)- and (3, 6)-regular SC-LDPC codes and (5, 10)- and (3, 6)-regular SC-LDPC codes, respectively.

D. Asymptotic Decoding Complexity Analysis

In this section, we analyze the asymptotic decoding complexity of the SC-RA based JSCAC scheme with partial expanding window decoding (PJEWD) by the proposed density evolution algorithm. Considering the decoding complexity of SC-RA based JSCAC with PJEWD scheme is related with the code parameters and channel conditions, etc., we could not describe it with a simple arithmetic expression. However, by counting the message updates Num_{me} during the density evolution process described in Section III-A, we can numerically analyze the asymptotic decoding complexity for any specific anytime $(Q^{sc}, A^{sc}, \lambda^{sc}, \gamma^{sc}, Q^{cc}, A^{cc}, \lambda^{cc}, \gamma^{cc})$ code.

Take the anytime (4, 12, 0.5, 3, 3, 3, 0.1, 3) code as an example, Fig. 9(a) and Fig. 9(b) describe its asymptotic decoding complexity as the decoding delay and channel conditions, respectively. Note that, the left y-axis indicates the average message updates normalized by the (3, 12)- and (3, 6)-regular LDPC based JSCC scheme [6] with the same maximum iteration number $i_{max} = 30$; and the right y-axis represents the message updates reduction ratio of the PJEWD scheme to the JEWD scheme. In Fig. 9(a), the growth rate of message updates as decoding delay of the proposed PJEWD scheme (blue line with square markers) is much slower than the conventional JEWD scheme (dark line with star markers). Moreover, the message updates reduction ratio of PJEWD scheme to JEWD scheme (red line with circle markers) increases sharply when the decoding delay is relatively small, and then gradually slows down as the increase of decoding delay. When the decoding delay is 1000, the reduction ratio is up to about 48%. Fig. 9(b) shows the decoding complexity as the channel condition with fixed chain lengths of 100 and 300.

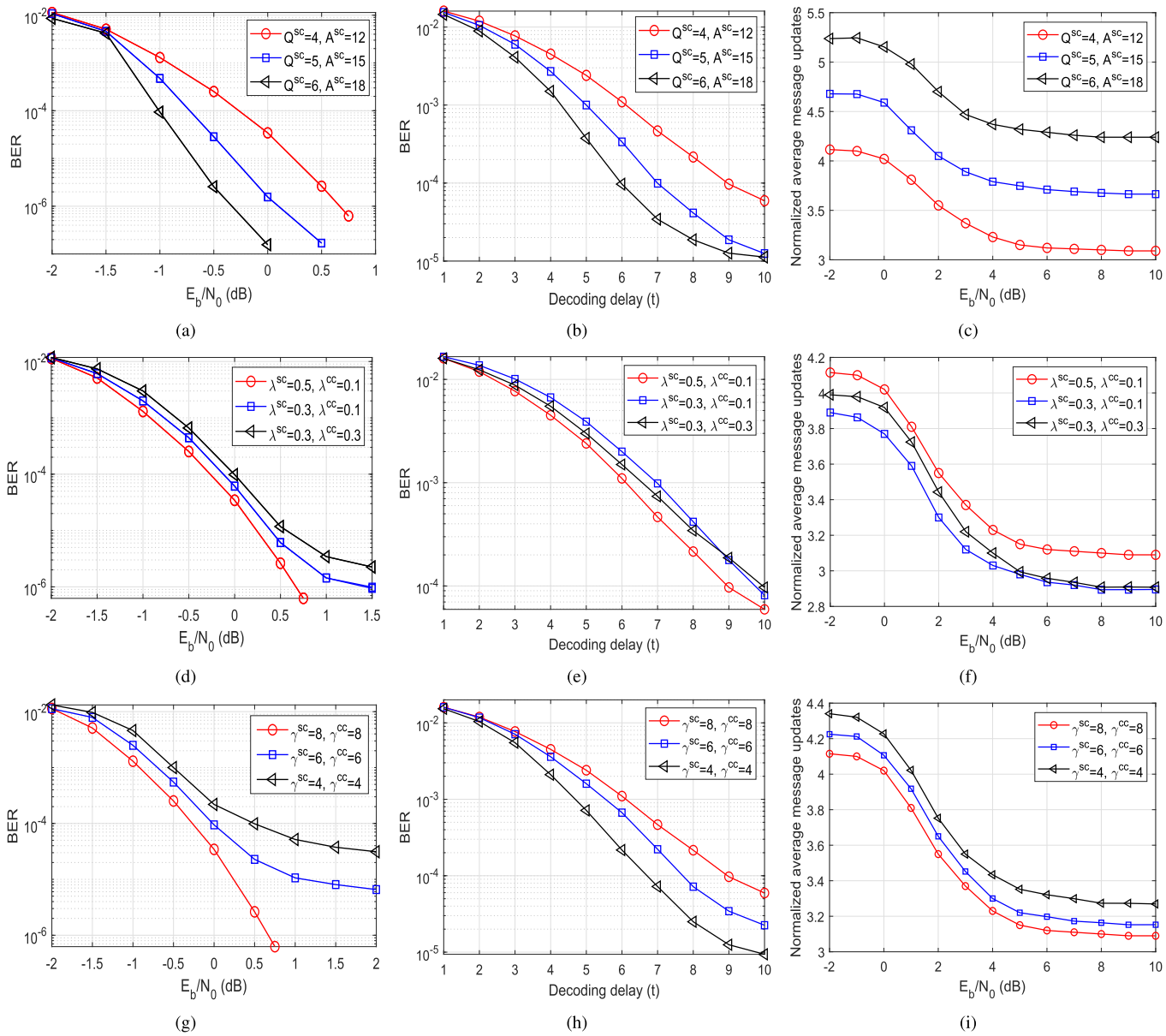

Fig. 10. Effects of code parameters with frame length of 1600 bits, $N_b^{cc} = 160$ and $p = 0.02$: (a) source node degree effect on BER performance; (b) source node degree effect on anytime property; (c) source node degree effect on average message updates; (d) exponential rate effect on BER performance; (e) exponential rate effect on anytime property; (f) exponential rate effect on average message updates; (g) coupling length effect on BER performance; (h) coupling length effect on anytime property; (i) coupling length effect on average message updates.

It can be seen that the decoding complexity is decreased as the channel condition becomes better. When the SNR is higher than 5 dB, the reduction ratio gradually stops increasing. For the chain length of $L = 100$, the normalized average message updates are close to the (3, 12)- and (3, 6)-regular LDPC based JSCC scheme, especially in the high SNR region.

To sum up, the decoding complexity of SC-RA based JSCAC with PJEWD scheme can be analyzed by the proposed DE algorithm with given code parameters, which can be substantially reduced compared to the traditional JEWD scheme.

IV. Finite-Length Performance of JSCAC Scheme

Numerical results are presented to verify the finite-length performances of the SC-RA based JSCAC scheme. We first discuss the effects of code parameters on the finite-length performance, and show the BER performance and decoding complexity of PJEWD scheme. Then we benchmark the proposed JSCAC scheme against the prior-art JSCC schemes [6], [7], [9], [12], [13], [14], [16], [17] on the source with the same frame length (or the equal *latency* defined in [16] and [17]). For SC-LDPC based JSCC scheme [16], [17] and the proposed SC-RA based JSCAC scheme, the maximum iteration number is set as $l_{\max} = 30$, and the block code rates are referred to in comparisons. Finally, we apply the proposed JSCAC scheme to the HSP finite-length source transmission and the source streaming scenarios.

A. Parameter Effects on the Finite-Length Performance

Fig. 10(a) to Fig. 10(c) show the effects of source node degrees with fixed $Q^{cc} = A^{cc} = 4$, $\lambda^{sc} = 0.5$, $\lambda^{cc} = 0.1$, $\gamma^{sc} = \gamma^{cc} = 8$, and $p = 0.02$. It can be seen that the largest

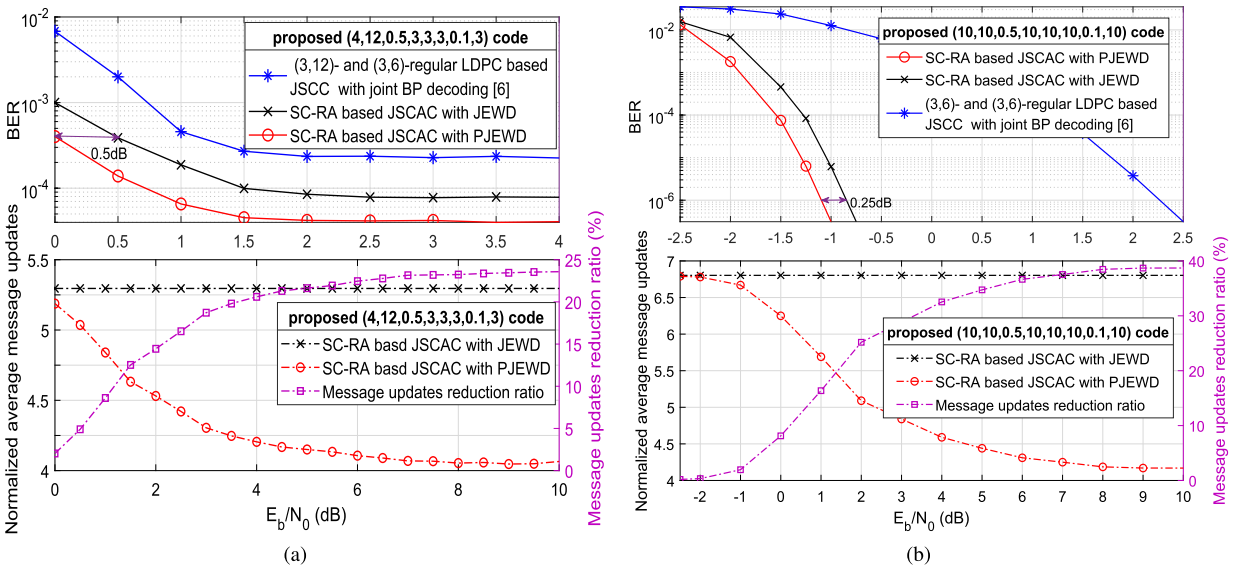

Fig. 11. Finite-length performance of PJEWD scheme: (a) the anytime (4, 12, 0.5, 3, 3, 3, 0.1, 3) code with frame length of 1600 bits, $R_b^{sc} = \frac{1}{4}$, $R_b^{cc} = \frac{1}{2}$, $p = 0.02$. The average message updates are normalized by the (3,12)- and (3,6)-regular LDPC based JSCC scheme [6]; (b) the anytime (10, 10, 0.5, 10, 10, 10, 0.1, 10) code with frame length of 3200 bits, $R_b^{sc} = \frac{1}{2}$, $R_b^{cc} = \frac{1}{2}$, $p = 0.04$. The average message updates are normalized by (3,6)- and (3,6)-regular LDPC based JSCC scheme [6].

source node degrees of $Q^{sc} = 6$ and $A^{sc} = 18$ can both attain the best error correction performance for the whole source frame, and the quickest decay rate of error probability for each block with $N_b^{cc} = 160$ bits at $\frac{E_b}{N_0} = -1$ dB (the same conditions in Fig. 10(e) and Fig. 10(h)). However, the largest node degrees also lead to the highest normalized average message updates.

Fig. 10(d) to Fig. 10(f) describe the effects of exponential rates with fixed $Q^{sc} = 4$, $A^{sc} = 12$, $Q^{cc} = 4$, $A^{cc} = 4$, $\gamma^{sc} = \gamma^{cc} = 8$, and $p = 0.02$. First, in Fig. 10(d), a larger λ^{sc} but a smaller λ^{cc} can achieve a better error correction performance, such as the red line with circle markers ($\lambda^{sc} = 0.5$, $\lambda^{cc} = 1$). Second, in Fig. 10(e), compared with the blue line with squared markers ($\lambda^{sc} = 0.3$, $\lambda^{cc} = 0.1$), both increasing λ^{sc} from 0.3 to 0.5 with fixed $\lambda^{cc} = 0.1$ (the red line with circle markers) and increasing λ^{cc} from 0.1 to 0.3 with fixed $\lambda^{sc} = 0.3$ (the black line with triangle markers) can accelerate the decay rate of error probability. Moreover, the effect of λ^{sc} is greater than λ^{cc}, which is consistent with the theoretical analysis. However, as seen in Fig. 10(f), a larger λ^{sc} or a larger λ^{cc} would also increase the decoding complexity. The code with $\lambda^{sc} = 0.5$ and $\lambda^{cc} = 1$ has the largest average message updates.

Fig. 10(g) to Fig. 10(i) indicate the effects of coupling lengths with $Q^{sc} = 4$, $A^{sc} = 12$, $Q^{cc} = 4$, $A^{cc} = 4$, $\lambda^{sc} = 0.5$, $\lambda^{cc} = 0.1$, $p = 0.02$. As in the theoretical analysis, the source and channel coupling lengths are set to be the same for easy storage. It can been seen that a smaller coupling length with lower BP decoding threshold would cause a higher error floor in the finite-length region (black line with triangle markers, $\gamma^{sc} = \gamma^{cc} = 4$). Moreover, it can also achieve the fastest decay rate of error probability but the largest average message updates.

To sum up, each code parameter has different effects on the finite-length performances. Therefore, we should choose the appropriate code parameters according to the specific requirements.

B. Finite-Length Performance of the PJEWD Scheme

Fig. 11 shows the finite-length performance of the SC-RA based JSCAC with PJEWD scheme on the error correction performance and the decoding complexity. We benchmark it with the SC-RA based JSCAC with JEWD scheme, and block regular LDPC code based JSCC schemes with joint BP decoding [6]. For all the compared schemes, the maximum iteration number is set as $l_{\max} = 30$, and no stopping rule is adopted during the decoding iterations.

In Fig. 11(a), the anytime (4, 12, 0.5, 3, 3, 3, 0.1, 3) code is adopted with the frame length of 1600 bits, $R_b^{sc} = \frac{1}{4}$, $R_b^{cc} = \frac{1}{2}$, $N_b^{cc} = 160$, $L = 10$, and $p = 0.02$. Specifically, we analyze the BER performance and the normalized average message updates. It can be seen that SC-RA based JSCAC with JEWD scheme can attain 0.5 dB decoding gains at the BER of 4×10^{-4} over the (3, 12)- and (3,6)-regular LDPC based JSCC scheme [6] with the price of about 5.29 times message updates per iterations. While the SC-RA based JSCAC with PJEWD scheme can further attain an extra 0.5 dB gains with message updates reduction ratio about 2.08% to 23.58% within the SNR region of $[0, 10]$ dB. Fig. 11(b) provides another example of anytime $(10, 10, 0.5, 10, 10, 10, 0.1, 10)$ code with $R_b^{sc} = \frac{1}{2}$ and $R_b^{cc} = \frac{1}{2}$, where the frame length of 3200 bits and $p = 0.04$. Considering the larger node degrees and coupling lengths of 10, the BER curves have early and sharp waterfall regions, and the PJEWD scheme can attain about 0.25 dB gains over the JEWD scheme at BER of 10^{-6}. While the normalized average message updates of PJEWD scheme is also reduced from 0.19% to 38.71% within the SNR of $[-2, 10]$ dB.

In conclusion, based on the observation of inconsistent convergence between the source and channel decoders, the

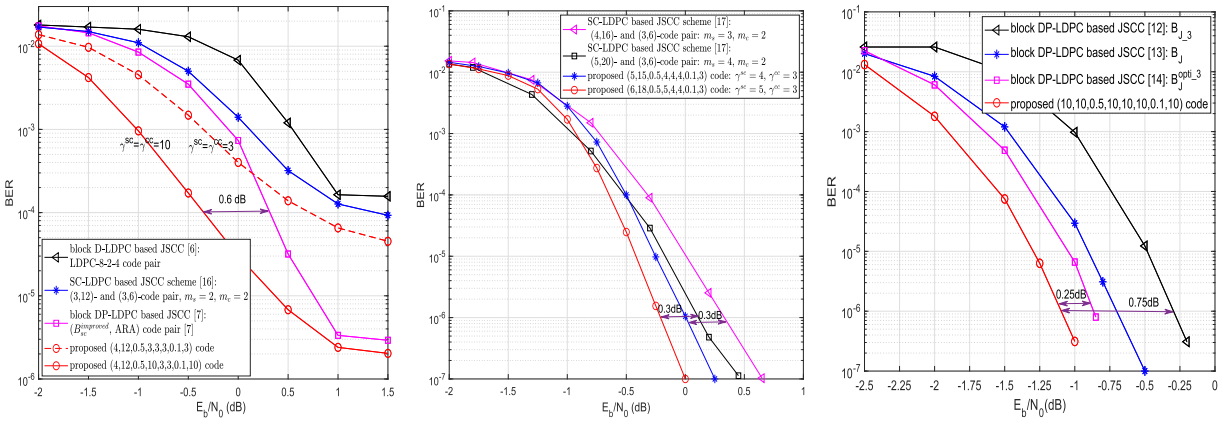

(a) (b) (c)

Fig. 12. Performance comparisons with prior-art JSCC schemes: (a) the frame length (or the equal *latency* in [16]) is 1600, and $R_b^{sc} = \frac{1}{4}$, $R_b^{cc} = \frac{1}{2}$, $p = 0.02$, $N_b^{cc} = 160$, $L = 10$ ($2M = 160$, $W = 10$ in [16]); (b) the frame length (or the equal *latency* in [17]) is 3200, $R_b^{sc} = \frac{1}{4}$, $R_b^{cc} = \frac{1}{2}$, $p = 0.02$, $N_b^{cc} = 400$, $L = 8$ ($2M = 400$, $W = 8$ in [17]); (c) the frame length is 3200, $R_b^{sc} = \frac{1}{2}$, $R_b^{cc} = \frac{1}{2}$, $p = 0.04$, $N_b^{cc} = 320$, $L = 10$.

partial updating strategies of the PJEWD scheme can not only reduce the decoding complexity but also prevent the error propagation, so as to improve the BER performance. Considering the short chain length, the finite-length performance is worse than the theoretical analysis results. Increasing the chain length is expected to narrow the gap.

C. Comparisons With Prior-Art JSCC Schemes

Fig. 12(a) shows the comparisons for the source with frame length of 1600 bits, the block length of $N_b^{cc} = 160$ bits, $L = 10$, $p = 0.02$, $R_b^{sc} = \frac{1}{4}$ and $R_b^{cc} = \frac{1}{2}$. It can be seen that the anytime $(4, 12, 0.5, 3, 3, 3, 0.1, 3)$ code with coupling lengths of $\gamma^{sc} = \gamma^{cc} = 3$ (red dashed line with circle markers) outperforms the block D-LDPC based JSCC scheme with regular LDPC-8-2-4 code pair (black line with triangle markers), as well as the (3, 12)- and (3, 6)-regular SC-LDPC based JSCC scheme with comparable memories of $m_s = m_c = 2$ (blue line with star markers) in both waterfall and error floor regions. As the coupling lengths increase to 10, the anytime $(4, 12, 0.5, 10, 3, 3, 0.1, 10)$ code (red solid line with circle markers) can achieve similar lower error floors about 10^{-6} with the block DP-LDPC based JSCC scheme in [7] with optimized $\mathbf{B}_{sc}^{improved}$ source code and ARA channel code as code pair (magenta line with square markers), and can attain about 0.6 dB gains at BER$= 10^{-4}$.

Fig. 12(b) compares the performances with the SC-LDPC based JSCC scheme in [17] with the frame length of 3200 bits and block length of $N_b^{cc} = 400$ bits. Compared to the (4, 16)- and (3, 6)-regular SC-LDPC codes with memories of $m_s = 3, m_c = 2$ in [17], the anytime (5, 15, 0.5, 4, 4, 4, 0.1, 3) code with similar node degrees and comparable coupling lengths of $\gamma^{sc} = 4, \gamma^{cc} = 3$ can achieve about 0.3 dB gains at BER$= 10^{-6}$. While the anytime (6, 18, 0.5, 5, 4, 4, 0.1, 3) code with increased source node degrees and coupling lengths of $\gamma^{sc} = 5, \gamma^{cc} = 3$ can further improve the performances, and also outperforms the (5, 20)- and (3, 6)-regular SC-LDPC codes with memories of $m_s = 4, m_c = 2$ about 0.3 dB.

Fig. 12(c) shows the performance comparisons with the latest block DP-LDPC based JSCC works [12], [13], [14], where the joint base matrix is designed with various optimization methods. The source probability is set as $p = 0.04$ and the encoded frame length is 3200 bits. The source and channel block code rate are set as $R_b^{sc} = \frac{1}{2}$ and $R_b^{cc} = \frac{1}{2}$, respectively. The chain length of anytime $(10, 10, 0.5, 10, 10, 10, 0.1, 10)$ code is $L = 10$. In Fig. 12(c), the anytime $(10, 10, 0.5, 10, 10, 10, 0.1, 10)$ code outperforms the compared DP-LDPC code $\mathbf{B}_{J\_3}$ [12] about 0.75 dB, and the optimized DP-LDPC code $\mathbf{B}_J^{opti\_3}$ [14] about 0.25 dB at the BER of 10^{-6}.

In summary, the good error correction performances of SC-RA based JSCAC with PJEWD scheme benchmarked against the prior-art JSCC schemes due to the following factors: 1) the good error correction performance of SC-RA codes; 2) the expanding window decoding structure of anytime coding techniques with good error correction performance but higher decoding complexity than the joint BP decoding and the sliding window decoding; 3) the novel partial updating strategies in the PJEWD scheme.

D. Application for Finite-Length HSP Source Transmission

This subsection discusses the error correction performance of the proposed JSCAC scheme for source with high source probability (HSP) and finite-length. Assuming that a source streaming produces message blocks with a fixed length of $N_b^{sc} = 320$ bits and the source block code rate of $R_b^{sc} = \frac{1}{4}$ (or $R_b^{sc} = \frac{1}{2}$), then the sub-blocks of encoded channel sequence have a block-length of $N_b^{cc} = 160$ (or $N_b^{cc} = 320$) bits with the channel block code rate of $R_b^{cc} = \frac{1}{2}$.

Fig. 13 shows the BER performance of the proposed JSCAC scheme for a single HSP message block in the source streaming against the decoding delay. In Fig. 13(a), the anytime $(4, 12, 0.5, 3, 3, 3, 0.1, 3)$ code with $\gamma^{sc} = \gamma^{cc} = 3$ (red lines with circle markers) and the anytime $(4, 12, 0.5, 10, 3, 3, 0.1, 10)$ code with $\gamma^{sc} = \gamma^{cc} = 10$ (blue lines with star markers) are adopted. The exponential rates of λ^{sc} and λ^{cc} are set to be 0.5 and 0.1, respectively. The source probabilities are set as $p = 0.02$ (solid lines) and $p = 0.03$ (dashed lines), respectively. It can be found that for the block DP-LDPC based JSCC scheme [7] with an

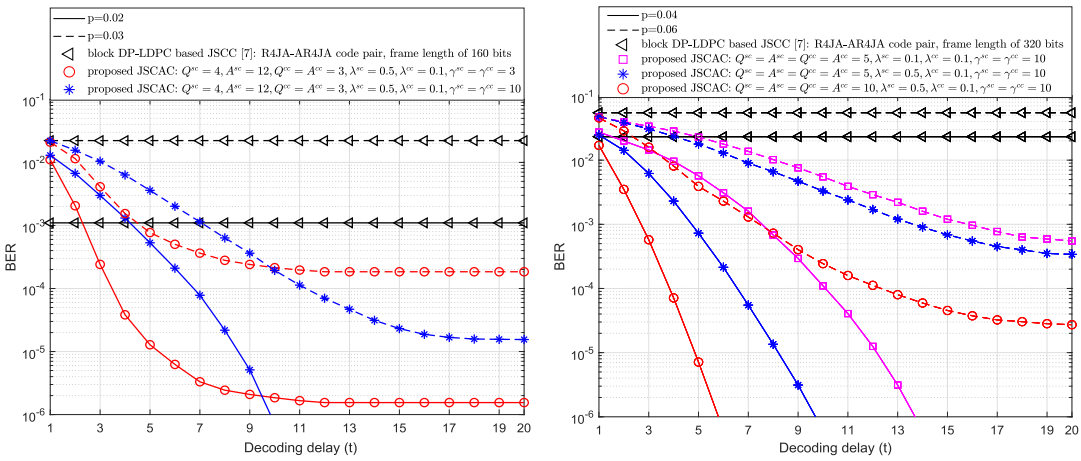

(a) (b)

Fig. 13. BER performance as a function of the decoding delay for the HSP source block bits versus the block DP-LDPC based JSCC scheme: (a) $R_b^{sc}=\frac{1}{4}$, $R_b^{cc}=\frac{1}{2}$, $p=0.02, 0.03$, $N_b^{cc}=160$, $\frac{E_b}{N_0}=2$ dB; (b) $R_b^{sc}=\frac{1}{2}$, $R_b^{cc}=\frac{1}{2}$, $p=0.04, 0.06$, $N_b^{cc}=320$, $\frac{E_b}{N_0}=-1.5$ dB.

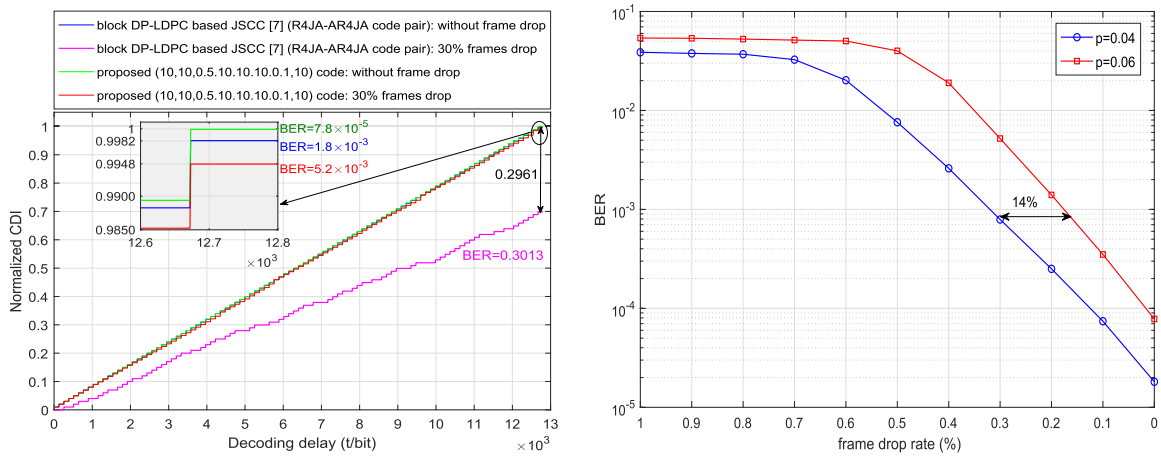

(a) (b)

Fig. 14. Performance comparisons on the jitter and jerkiness reduction in source streaming scenarios with $N_b^{sc}=64$ bits, $L=100$, $R_b^{sc}=\frac{1}{2}$, $R_b^{cc}=\frac{1}{2}$, $\frac{E_b}{N_0}=2$ dB: (a) normalized cumulative number of correctly decoded information bits (CDI) for the source streaming with and without frame drop; (b) BER performance of the anytime $(10, 10, 0.5, 10, 10, 10, 0.1, 10)$ code with different p as the frame drop rate.

encoded frame length of 160 bits, where rate-$\frac{1}{4}$ R4JA and rate-$\frac{1}{2}$ AR4JA codes are used as the source-channel code pair, the BERs would not change with the decoding delay, which suffers from high error floors for sources with high source probabilities of $p=0.02$ ($p=0.03$)[1] and finite source block-length of 160 bits. For the proposed codes, the early transmitted HSP blocks that are not fully corrected are likely to be recovered in the latter time slots. The BER curve of anytime $(4, 12, 0.5, 3, 3, 3, 0.1, 3)$ code approaches to 10^{-6} and 10^{-4} within the decoding delay of $t=10$ and $t=12$ for source blocks with $p=0.02$ and $p=0.03$, respectively. Comparing with the $(4, 12, 0.5, 3, 3, 3, 0.1, 3)$ code, the BER curve of $(4, 12, 0.5, 10, 3, 3, 0.1, 10)$ with coupling length of 10 has lower error floors but smaller slope. Proper coupling length could trade off the performance of the two aspects.

Fig. 13(b) provides another example with $R_b^{sc}=\frac{1}{2}$, $R_b^{cc}=\frac{1}{2}$, $N_b^{cc}=320$ bits. For $p=0.04$, compared with the anytime (5, 5, 0.1, 10, 5, 5, 0.1, 10) code (magenta solid line with square markers), the anytime (5, 5, 0.5, 10, 5, 5, 0.1, 10) code with greater $\lambda^{sc}=0.5$ (blue solid line with star markers) has a larger slope at the waterfall region. Moreover, the anytime (10, 10, 0.5, 10, 10, 10, 0.1, 10) code with greater node degrees of 10 (red solid line with circle markers) can further increase the slope value. For a larger p of 0.06 (dotted line), the BER curves decline slowly and gradually flatten out. Thereinto, the anytime (5, 5, 0.1, 10, 5, 5, 0.1, 10) code and the anytime (5, 5, 0.5, 10, 5, 5, 0.1, 10) code has similar error floors of BER$=4\times10^{-4}$, while the anytime (10, 10, 0.5, 10, 10, 10, 0.1, 10) code has a lower error floor about BER$=3\times10^{-5}$. That is to say, the effects of increasing node degrees is more powerful than increasing λ^{sc} on reducing the error floor.

To conclude, the above cases verify the effectiveness of proposed JSCAC scheme on the finite-length HSP source transmission, which is a tough issue for the traditional JSCC systems. The performance gains are due to the anytime coding techniques with relatively higher decoding complexity compared with the joint BP decoding of JSCC schemes, which can be significantly reduced by improving the decoding strategies.

[1]The asymptotic source decoding thresholds of the rate-$\frac{1}{4}$ R4JA code and rate-$\frac{1}{2}$ R4JA code are $p=0.019$ and $p=0.069$, respectively [34].

E. Application in the Source Streaming Scenarios

Finally, we apply the proposed JSCAC scheme to the source streaming scenarios. We focus on restraining the jitter and jerkiness caused by frame drops due to the transmission errors. The encoding and decoding mechanisms of the proposed JSCAC scheme can effectively recover the dropped frames, which is not achievable by traditional JSCC schemes.

In the simulation, a source streaming produces message blocks with a fixed short length of $N_b^{sc} = 64$ bits and an average source probability of $p = 0.06$. The source and channel block code rates are set as $R_b^{sc} = \frac{1}{2}$ and $R_b^{cc} = \frac{1}{2}$, respectively, and the chain length is $L = 100$. In order to elaborately show the recovering process of the proposed code for the dropped frames, we track the Cumulative number of correctly Decoded Information bits (CDI) as a function of the decoding delay (in unit of bits), and benchmark it against the block DP-LDPC based JSCC scheme with R4JA-AR4JA code pair. The $\frac{E_b}{N_0}$ is set as good as 2 dB in order to better evaluate the affects of the proposed code on the dropped frames. As seen in Fig. 14(a), for the situation without frame drop, the anytime $(10, 10, 0.5, 10, 10, 10, 0.1, 10)$ code can achieve a lower error floor of BER$= 7.8 \times 10^{-5}$ for short HSP source blocks with $N_b^{sc} = 64$ bits and $p = 0.06$. For the situation with 30% frames drop, the anytime $(10, 10, 0.5, 10, 10, 10, 0.1, 10)$ code can recover the best part of dropped frames and obtain similar BER performance with that of the block DP-LDPC based JSCC scheme without frame drop. Moreover, the normalized CDI gains of the proposed code over the block DP-LDPC based JSCC scheme with frame drop is 0.2961.

Fig. 14(b) shows the BER performance of the anytime $(10, 10, 0.5, 10, 10, 10, 0.1, 10)$ code for the source streaming as the frame drop rate is decreased. It can be observed that, the decoding waterfall begins at the frame drop rate of 60% and 70% for $p = 0.06$ and $p = 0.04$, respectively. A reliable transmission performance can be attained with the frame drop rate lower than 30%, and the BER curve of $p = 0.04$ has about 14% drop rate gains over that of $p = 0.06$ at BER $= 7.9 \times 10^{-4}$.

To summarize, the proposed JSCAC scheme is capable of restraining the jitter and jerkiness in the source streaming. The performance gains on recovering the dropped frames over the block code based JSCC scheme are attained by trading off with the decoding latency.

V. Conclusion

This paper has made a comprehensive theoretical analysis for the joint source channel anytime coding (JSCAC) scheme with the partial joint expanding window decoding (PJEWD) based on the density evolution, including the asymptotic anytime property, the decoding threshold, and the decoding complexity. A comprehensive study of the design parameters both in asymptotic and finite-length regions has also been performed. Compared with the prior-art joint source channel coding (JSCC) schemes, the JSCAC scheme has pursued a low latency and high reliability transmission at the cost of relatively high decoding complexity. Moreover, the improved PJEWD algorithm has tactfully reduced the decoding complexity of traditional expanding window decoding while improved the error correction performance. With an acceptable decoding complexity, the proposed JSCAC scheme has provided new perspectives to resolve the finite-length HSP source transmission issue in the JSCC system, as well as the jitter and jerkiness reduction in the source streaming scenarios. On the other hand, the proposed density evolution algorithm has provided a good inspiration and reference for the analysis of similar JSCAC systems, which is also helpful for us to work on the code optimization in the next research.

Appendix

A. Supporting Argument for Eq.(16) and Claim (a) in Section III-B

We first derived that $x_{cv}^{\infty}(i_c, t) = +\infty$, $\forall 0 < i_c \leq t$, $\frac{E_b}{N_0} > \frac{E_b}{N_0}^*$. The DE equation of $y_{cv}^{l}(j_c, t)$ becomes as follows when we combine (8) and (9) into (6):

$$\begin{aligned} & y_{cv}^{l}(j_c, t) \\ & = \Phi^{-1}\Bigg\{1 - \Bigg[1 - \Phi\Bigg(J^{-1}\Bigg(\sum_{k=0}^{\infty} P_r^{cc}(k) J\Big(\mu_0 + (Q^{cc} - 1) \\ & \quad \cdot J^{-1}\Big(\sum_{j_c'=0}^{t-j_c+k} P_r^{cc}(j_c') J\Big(y_{cv}^{l-1}(j_c - k + j_c', t)\Big)\Big) \\ & \quad + J^{-1}\Big(J\big(\tilde{y}_{sv}^{l-1}(j_s, t)\big)\Big)\Big)\Bigg)\Bigg]^{A^{cc}-1} \\ & \quad \cdot \Big[1 - \Phi\Big(\mu_0 + y_{cp}^{l-1}(j_c, t)\Big)\Big]^2\Bigg\} \end{aligned} \tag{25}$$

We rewrite (25) as below to simplify the symbolic representation.

$$t^l = f(s, t^{l-1}, \gamma^{l-1}, \delta^{l-1}), \tag{26}$$

where $t^l = y_{cv}^{l}(j_c, t)$, $s = \mu_0 = \frac{2}{\sigma_n^2}$, $t^{l-1} = y_{cv}^{l-1}(j_c, t)$, $\gamma^{l-1} = \tilde{y}_{sv}^{l-1}(j_s, t)$, $\delta^{l-1} = \tilde{y}_{cp}^{l-1}(j_c, t)$. The initial values are $t^0 = \gamma^0 = \delta^0 = 0$. Since $t^1 = f(s, 0, 0, 0) > 0$ for $s > 0$, the iteration of (26) will always start. Note that $f(\cdot)$ is a multivariate function of t^{l-1}, γ^{l-1}, and δ^{l-1}. While in the partial derivative direction of t^{l-1}, $f(\cdot)$ can be considered as a unary function dominated by t^{l-1}. Since the functions $\Phi(t^{l-1})$ and $\Phi^{-1}(t^{l-1})$ are monotonically decreasing while the functions $J(t^{l-1})$ and $J^{-1}(t^{l-1})$ are monotonically increasing on $0 < t^{l-1} < +\infty$. We conclude that $t^l = f(s, t^{l-1}, \gamma^{l-1}, \delta^{l-1})$ is monotonically increasing on the partial derivative direction of t^{l-1}, for $0 < s < +\infty$, $0 < t^{l-1} < +\infty$. According to Lemma 2 in [31], we conclude that for $s > s^*$ (or $\frac{E_b}{N_0} > \frac{E_b}{N_0}^*$), $t^l(s) > t^l(s^*)$ and $t^l(s)$ will converge to $+\infty$ as $l \to +\infty$. Lemma 2 in [31] is cited as below:

Lemma 2: $t^l(s)$ will converge to $+\infty$ iff $t < f(s, t)$ for all $t \in \mathbb{R}^+$ [31].

Proof: Let us first assume $t < f(s, t), \forall t \in \mathbb{R}^+$. Since $t^{l+1} > t^l$, t^l will converge to $t^{+\infty} \in (0, +\infty]$. However, $t^{+\infty}$ cannot be finite, because if so then $t^{+\infty} = f(s, t^{+\infty})$. Now we assume $t' = f(s, t')$ for some $t' \in \mathbb{R}^+$. $t' \neq 0$ because $f(s, 0) > 0$. Since $f(\cdot)$ is continuous, there exists $t_0 > 0$ such

that $t < f(s,t)$ *for* $\forall t \in (0, t_0)$. *Now we choose the smallest* $t' \in \mathbb{R}^+$ *such that* $t' = f(s,t')$ *and* $t < f(s,t)$ *for* $\forall t \in (0,t')$. *Since* $0 < f(s,0) < f(s,t') = t'$ *and* $f(s,t) < f(s,t') = t'$ *for* $\forall t \in (0,t')$, *we conclude that* $t^l < t'$ *for* $\forall l \geq 0$. ■

Correspondingly, when t^l (i.e. $y_{cv}^l(j_c,t)$) converges to $+\infty$ for $\frac{E_b}{N_0} > \frac{E_b}{N_0}^*$ as $l \to \infty$, the DE equation (9) for $x_{cv}^{l+1}(i_c,t)$ becomes as:

$$x_{cv}^{\infty}(i_c,t) = \mu_0 + (Q^{cc}-1)\cdot J^{-1}\Big(\sum_{j_c=0}^{t-i_c} P_r^{cc}(j_c) J\big(+\infty\big)\Big) + J^{-1}\Big(J\big(\tilde{y}_{sv}^l(j_s,t)\big)\Big) = +\infty. \quad (27)$$

With the similar derivation process, we can also conclude the results that $x_{sv}^{\infty}(i_s,t) = +\infty$, $x_{cp}^{\infty}(j_c,t) = +\infty$, $x_{sp}^{\infty}(j_s,t) = +\infty$, $\forall 0 < i_s, j_c, j_s \leq t$, $\frac{E_b}{N_0} > \frac{E_b}{N_0}^*$. ■

ACKNOWLEDGMENT

This article was produced by the IEEE Publication Technology Group, Piscataway, NJ.

REFERENCES

[1] J. L. Massey, "Joint source and channel coding," in *Communications Systems and Random Process Theory*, vol. 11. Alphen aan den Rijn, The Netherlands: Sijthoff & Noordhoff, 1978, pp. 279–293.

[2] T. Ancheta, "Syndrome-source-coding and its universal generalization," *IEEE Trans. Inf. Theory*, vol. AP-22, no. 4, pp. 432–436, Jul. 1976.

[3] A. Sahai and S. Mitter, "The necessity and sufficiency of anytime capacity for stabilization of a linear system over a noisy communication link—Part I: Scalar systems," *IEEE Trans. Inf. Theory*, vol. 52, no. 8, pp. 3369–3395, Aug. 2006.

[4] L. Grosjean, "Practical anytime codes," Ph.D. dissertation, KTH Roy. Inst. Technol., Stockholm, Sweden, 2016.

[5] C. E. Shannon, "A mathematical theory of communication," *Bell Syst. Tech. J.*, vol. 27, no. 3, pp. 379–423, Jul. 1948.

[6] M. Fresia, F. Perez-Cruz, H. V. Poor, and S. Verdu, "Joint source and channel coding," *IEEE Signal Process. Mag.*, vol. 27, no. 6, pp. 104–113, Nov. 2010.

[7] J. He, L. Wang, and P. Chen, "A joint source and channel coding scheme base on simple protograph structured codes," in *Proc. Int. Symp. Commun. Inf. Technol. (ISCIT)*, Oct. 2012, pp. 65–69.

[8] D. Divsalar, S. Dolinar, C. Jones, and K. Andrews, "Capacity-approaching protograph codes," *IEEE J. Sel. Areas Commun.*, vol. 27, no. 6, pp. 876–888, Aug. 2009.

[9] Q. Chen, L. Wang, S. Hong, and Z. Xiong, "Performance improvement of JSCC scheme through redesigning channel code," *IEEE Commun. Lett.*, vol. 20, no. 6, pp. 1088–1091, Jun. 2016.

[10] S. Hong, Q. Chen, and L. Wang, "Performance analysis and optimisation for edge connection of JSCC system based on double protograph LDPC codes," *IET Commun.*, vol. 12, no. 2, pp. 214–219, Jan. 2018.

[11] C. Chen, L. Wang, and S. Liu, "The design of protograph LDPC codes as source codes in a JSCC system," *IEEE Commun. Lett.*, vol. 22, no. 4, pp. 672–675, Apr. 2018.

[12] C. Chen, L. Wang, and F. C. M. Lau, "Joint optimization of protograph LDPC code pair for joint source and channel coding," *IEEE Trans. Commun.*, vol. 66, no. 8, pp. 3255–3267, Aug. 2018.

[13] Q. Chen, L. Wang, S. Hong, and Y. Chen, "Integrated design of JSCC scheme based on double protograph LDPC codes system," *IEEE Commun. Lett.*, vol. 23, no. 2, pp. 218–221, Feb. 2019.

[14] S. Liu, L. Wang, J. Chen, and S. Hong, "Joint component design for the JSCC system based on DP-LDPC codes," *IEEE Trans. Commun.*, vol. 68, no. 9, pp. 5808–5818, Sep. 2020.

[15] Q. Chen, F. C. M. Lau, H. Wu, and C. Chen, "Analysis and improvement of error-floor performance for JSCC scheme based on double protograph LDPC codes," *IEEE Trans. Veh. Technol.*, vol. 69, no. 12, pp. 14316–14329, Dec. 2020.

[16] A. Golmohammadi and D. G. M. Mitchell, "Concatenated spatially coupled LDPC codes for joint source-channel coding," in *Proc. IEEE Int. Symp. Inf. Theory (ISIT)*, Jun. 2018, pp. 631–635.

[17] A. Golmohammadi and D. G. M. Mitchell, "Concatenated spatially coupled LDPC codes with sliding window decoding for joint source-channel coding," *IEEE Trans. Commun.*, vol. 70, no. 2, pp. 851–864, Feb. 2022.

[18] A. Sahai, "Anytime information theory," Ph.D. dissertation, Dept. Elect. Eng. Comput. Sci., Massachusetts Inst. Technol., Cambridge, MA, USA, Apr. 2001.

[19] H. Simsek, *Anytime Channel Coding With Feedback*. Berkley, CA, USA: Univ. California Press, 2004.

[20] R. T. Sukhavasi and B. Hassibi, "Linear error correcting codes with anytime reliability," in *Proc. IEEE Int. Symp. Inf. Theory*, Jul. 2011, pp. 1748–1752.

[21] L. Dössel, L. K. Rasmussen, R. Thobaben, and M. Skoglund, "Anytime reliability of systematic LDPC convolutional codes," in *Proc. IEEE Int. Conf. Commun. (ICC)*, Jun. 2012, pp. 2171–2175.

[22] L. Grosjean, L. K. Rasmussen, R. Thobaben, and M. Skoglund, "Systematic LDPC convolutional codes: Asymptotic and finite-length anytime properties," *IEEE Trans. Commun.*, vol. 62, no. 12, pp. 4165–4183, Dec. 2014.

[23] N. Zhang, M. Noor-A-Rahim, B. N. Vellambi, and K. D. Nguyen, "Anytime characteristics of protograph-based LDPC convolutional codes," *IEEE Trans. Commun.*, vol. 64, no. 10, pp. 4057–4069, Oct. 2016.

[24] M. Noor-A-Rahim, K. D. Nguyen, and G. Lechner, "Anytime reliability of spatially coupled codes," *IEEE Trans. Commun.*, vol. 63, no. 4, pp. 1069–1080, Apr. 2015.

[25] N. Zhang, M. Noor-A-Rahim, B. N. Vellambi, and K. D. Nguyen, "Anytime properties of protograph-based repeat-accumulate codes," in *Proc. IEEE Inf. Theory Workshop-Fall (ITW)*, Oct. 2015, pp. 177–181.

[26] M. Noor-A-Rahim, M. O. Khyam, Y. L. Guan, G. G. M. N. Ali, K. D. Nguyen, and G. Lechner, "Delay-universal channel coding with feedback," *IEEE Access*, vol. 6, pp. 37918–37931, 2018.

[27] L. Deng, Y. Wang, X. Yu, M. Noor-A-Rahim, Y. L. Guan, and Z. Shi, "Joint source channel anytime coding," in *Proc. IEEE Global Commun. Conf.*, Dec. 2020, pp. 1–6.

[28] M. Noor-A-Rahim, G. Lechner, and K. D. Nguyen, "Density evolution analysis of spatially coupled LDPC codes over BIAWGN channel," in *Proc. Austral. Commun. Theory Workshop (AusCTW)*, Jan. 2016, pp. 13–17.

[29] S. Johnson and G. Lechner, "Spatially coupled repeat-accumulate codes," *IEEE Commun. Lett.*, vol. 17, no. 2, pp. 373–376, Feb. 2013.

[30] Z. Xu, L. Wang, S. Hong, F. C. M. Lau, and C.-W. Sham, "Joint shuffled scheduling decoding algorithm for DP-LDPC codes-based JSCC systems," *IEEE Wireless Commun. Lett.*, vol. 8, no. 6, pp. 1696–1699, Dec. 2019.

[31] S.-Y. Chung, T. J. Richardson, and R. L. Urbanke, "Analysis of sum-product decoding of low-density parity-check codes using a Gaussian approximation," *IEEE Trans. Inf. Theory*, vol. 47, no. 2, pp. 657–670, Mar. 2001.

[32] S. T. Brink, G. Kramer, and A. Ashikhmin, "Design of low-density parity-check codes for modulation and detection," *IEEE Trans. Commun.*, vol. 52, no. 4, pp. 670–678, Apr. 2004.

[33] F. Cabarcas, R. D. Souza, and J. Garcia-Frias, "Turbo coding of strongly nonuniform memoryless sources with unequal energy allocation and PAM signaling," *IEEE Trans. Signal Process.*, vol. 54, no. 5, pp. 1942–1946, May 2006.

[34] C. Chen, L. Wang, and Z. Xiong, "Matching criterion between source statistics and source coding rate," *IEEE Commun. Lett.*, vol. 19, no. 9, pp. 1504–1507, Sep. 2015.

Li Deng received the Ph.D. degree from the National Key Laboratory of Wireless Communications, University of Electronic Science and Technology of China, in 2021. From 2019 to 2020, she was a Visiting Scholar with the School of Electrical and Electronic Engineering, Nanyang Technological University, Singapore. She is currently a Post-Doctoral Research Fellow with the University of Electronic Science and Technology of China. She is also a Professor with the School of Electronic Information and Automation, Guilin University of Aerospace Technology. Her current research interests include information and coding theory, DNA data storage, and image communication.

Xiaoxi Yu received the B.Eng. degree in electrical and electronics engineering and the M.S. degree in wireless communications and signal processing from the University of Bristol, in September 2016 and February 2018, respectively. She is currently pursuing the Ph.D. degree with Nanyang Technological University, Singapore. Her current research interests include information and coding theory and LDPC/protograph codes.

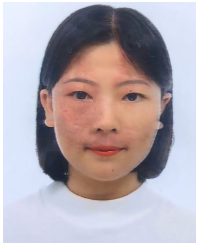

Yixin Wang received the Ph.D. degree from Nanyang Technological University (NTU), Singapore, in 2022. She joined A*STAR, Singapore, as a Research Scientist. Her current research interests include coding for DNA data storage, constrained codes, error control codes, and intelligent transport systems.

Md. Noor-A-Rahim received the Ph.D. degree from the Institute for Telecommunications Research, University of South Australia, Adelaide, SA, Australia, in 2015. He was a Post-Doctoral Research Fellow with the Centre for Infocomm Technology (INFINITUS), Nanyang Technological University (NTU), Singapore. He is currently a Senior Researcher with the School of Computer Science and Information Technology, University College Cork, Ireland. His current research interests include intelligent transportation systems, machine learning, the Internet of Things, and signal processing. He was a recipient of the Michael Miller Medal from the Institute for Telecommunications Research (ITR), University of South Australia, for the Most Outstanding Ph.D. Thesis in 2015.

Yong Liang Guan (Senior Member, IEEE) received the B.Eng. degree (Hons.) from the National University of Singapore and the Ph.D. degree from Imperial College London, U.K. He is currently a Professor of communication engineering with the School of Electrical and Electronic Engineering, Nanyang Technological University (NTU), Singapore, where he leads the Continental-NTU Corporate Research Laboratory and led the successful deployment of the campus-wide NTU-NXP V2X Test Bed. He has published an invited monograph, two books, and more than 450 journals and conference papers. He has secured more than $70 million of external research funding. He has 15 filed patents and three granted patents, one of which was licensed to NXP Semiconductors. His current research interests include coding and signal processing for communication systems and data storage systems. He is an Editor of the IEEE TRANSACTIONS ON VEHICULAR TECHNOLOGY. Currently, he is an Associate Vice President of NTU and a Distinguished Lecturer of the IEEE Vehicular Technology Society.

Zhiping Shi (Member, IEEE) received the master's and Ph.D. degrees from Southwest Jiaotong University, Chengdu, China, in 1998 and 2005, respectively. She was a Post-Doctoral Researcher with the University of Electronic Science and Technology of China (UESTC) from 2005 to 2007. From 2009 to 2010, she was a Visiting Scholar with Lehigh University, PA, USA. In 2007, she joined the School of Communication and Information, UESTC. Currently, she is a Professor with the National Key Laboratory of Communications, UESTC. Her current research interests include coding theory, cognitive radio, and wireless communication.

Zhongpei Zhang (Member, IEEE) received the B.S. and M.S. degrees from the Department of Physics, Sichuan Normal University, in 1990 and 1993, respectively, and the Ph.D. degree from the School of Computer and Communication Engineering, Southwest Jiaotong University, in 2000. From 2001 to 2003, he was a Post-Doctoral Fellow with the National Key Laboratory of Microwave and Digital Communication, Tsinghua University. From 2004 to 2005, he was a Post-Doctoral Fellow with the University of Oulu. He is currently a Professor and a Doctoral Tutor with the University of Electronic Science and Technology of China and the Shenzhen Institute for Advanced Study, University of Electronic Science and Technology of China. He has participated in many research projects and chaired the National High-Tech Research and Development Program of China (863 Program) on Coordinated Multiple Points Transmission and the National Natural Science Foundation of China on Massive MIMO Channel Acquisition. He has authored or coauthored more than 90 journal articles and conference papers. His current research interests include channel coding, coordinated multiple points transmission, information theory, channel estimation based on compressive sensing, reconfigurable-reflecting-surface aided communications, and joint sensing and communication.